Fundamentals of Automobile Handling Analysis

By D.H. Iacovoni

March 1969

EDC Library Ref. No. 1108

DISCLAIMER

FUNDAMENTALS OF AUTOMOBILE HANDLING ANALYSIS

by
D. H. Iacovoni

A paper to be presented to the Detroit Section
SAE Junior Activity Spring Lecture Series

March 13, 1969

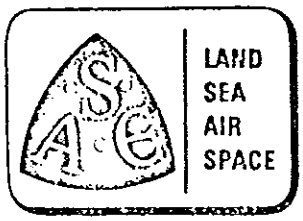

Society of Automotive Engineers, Inc.

FUNDAMENTALS OF AUTOMOBILE HANDLING ANALYSIS

INTRODUCTION

The term "handling," as used in this paper, refers to the task of controlling the path and speed of the vehicle. The general objective of handling research is to develop analytical and/or experimental tools for the design and development of a vehicle's handling qualities.

The general procedure that is followed in the pursuit of this objective is as follows:

- Develop mathematical and/or experimental techniques for predicting and measuring vehicle motion behavior under various types of inputs.
- Use these techniques to derive a fundamental understanding of vehicle motion behavior.
- Develop indexes of system performance that can be used in quantitatively defining vehicle response.
- Develop methods for relating these indexes of system performance to subjective opinion and/or vehicle-driver system performance.
- Establish system performance specifications for various types of vehicles in terms of the derived indexes of vehicle system performance.

For the study of handling, the vehicle-driver system is schematically presented in Figure 1. As shown, the system is essentially comprised of five basic elements, the driver, power train, braking, steering, and vehicle systems. The motion or path of the vehicle results from control inputs and/or disturbance inputs. The driver introduces control inputs into the various subsystems to achieve his desired maneuver. These inputs are influenced by environmental conditions and the feedbacks that the driver receives from the various systems. These

VEHICLE DRIVER SYSTEM DESCRIPTION

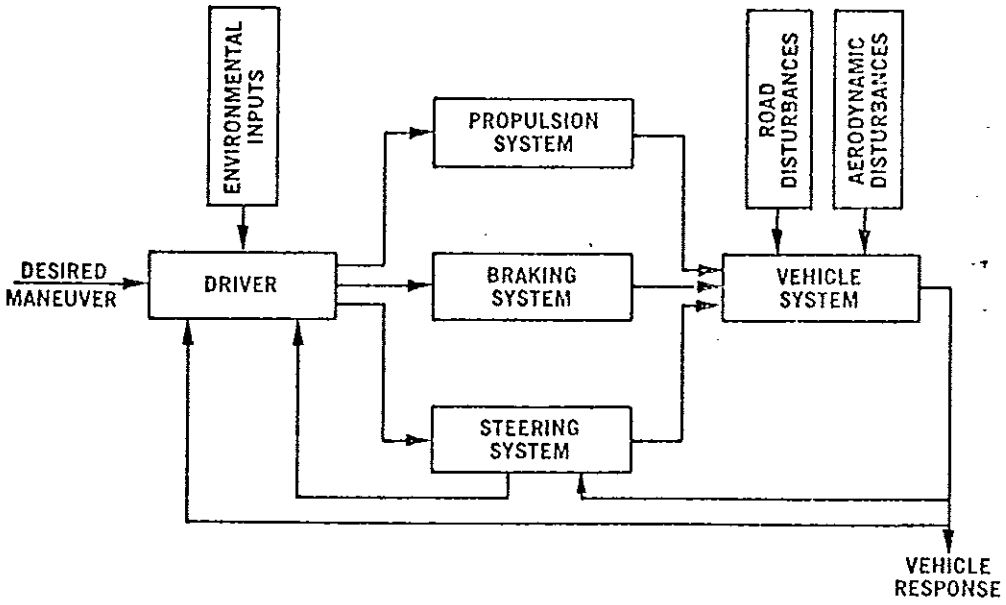

Figure 1

feedbacks signal him to make corrections in path caused by external wind or road disturbances. In effect the vehicle-driver system is a closed loop control system, in which the driver is both the error sensing mechanism and the controlling element.

The analysis of a closed loop control system requires knowledge of the dynamic characteristics of each element and the relation of each element to the whole system.

The driver, of course, is the most difficult element to define. Some success has been achieved (1, 2, 3, 4,) but to date the state of the art of simulating the vehicle-driver system as a closed loop control system for various maneuvering conditions is in a basic research stage.

The elements other than the human can be simulated and analyzed by well established methods of classical mechanics and control theory.

The past ten years has seen a rapid growth in the development of mathematical simulations and their use in general analytical investigations. The degree of sophistication in mathematical simulations has advanced to the point where almost any type of vehicle control or disturbance input can now be simulated. These simulations and related studies have significantly advanced the basic understanding of vehicle motion phenomena.

Despite all the sophistication in prediction techniques, however, the ability to define qualitative levels of handling performance with computed response characteristics is still lacking. This lack is due, in part, to the limited use of these techniques in the actual design process. This utilization has been hampered by the complex nature of the problem and the natural evolution that is required for the conversion of newly developed technology into practical analytical design tools. As these analytical tools become more widely used in actual design problems, a background of much needed numerical data generated for the various performance indexes will accrue. These values will take on increased significance as they are related to the varying types of vehicle behavior that are experienced by the design and development engineer in the normal course of his job.

The next phase of handling research therefore, should see increased emphasis on evolving simplified numerical measures (indexes of system performance) of various types of vehicle motion behavior, as well as the utilization of these measures in the actual design and development process.

The objective of this paper is to acquaint the novice with the fundamentals of handling analysis. The general procedure for developing a mathematical model will be described by developing the equations of motion for a simplified two degree of freedom model. Steady state and transient performance indexes that have been found useful in design and development will be described along with specific example applications.

DEVELOPMENT OF A MATHEMATICAL MODEL

Figure 2 describes the axis system and motion variables that are used in handling analysis.

As shown, the sprung mass of a vehicle can have six degrees of freedom: 3 translational and 3 rotational. The motion is usually considered in two modes: a stability and control mode and a performance and ride mode. The stability and control mode consists of yaw, roll, and sideslip, which are the motions that are principally excited by steering and/or wind disturbance inputs. The performance and ride mode consist of longitudinal, vertical, and pitch motions which result primarily from fore and aft traction and braking forces and vertical road disturbance inputs. Interactions exist between the two modes, due to suspension and steering kinematics, but these interactions are usually of a secondary nature.

The first step in the development of a mathematical model is to construct a free body diagram of the vehicle as shown in Figure 3.

It is assumed that the vehicle travels at a constant forward speed and can only yaw (rotation about the vertical z axis) and sideslip (lateral translation along the y axis). It is also assumed that the right and left tires have identical cornering properties and can be represented by a single tire having the combined properties.

The next step is to equate the inertial forces and moments to their respective external forces and moments. If all six degrees of freedom were to be considered, there would have to be 6 equations of equilibrium, 3 force and 3 moment equations. Because this development considers only yaw and sideslip, only 2 equations are needed,

VEHICLE AXIS SYSTEM

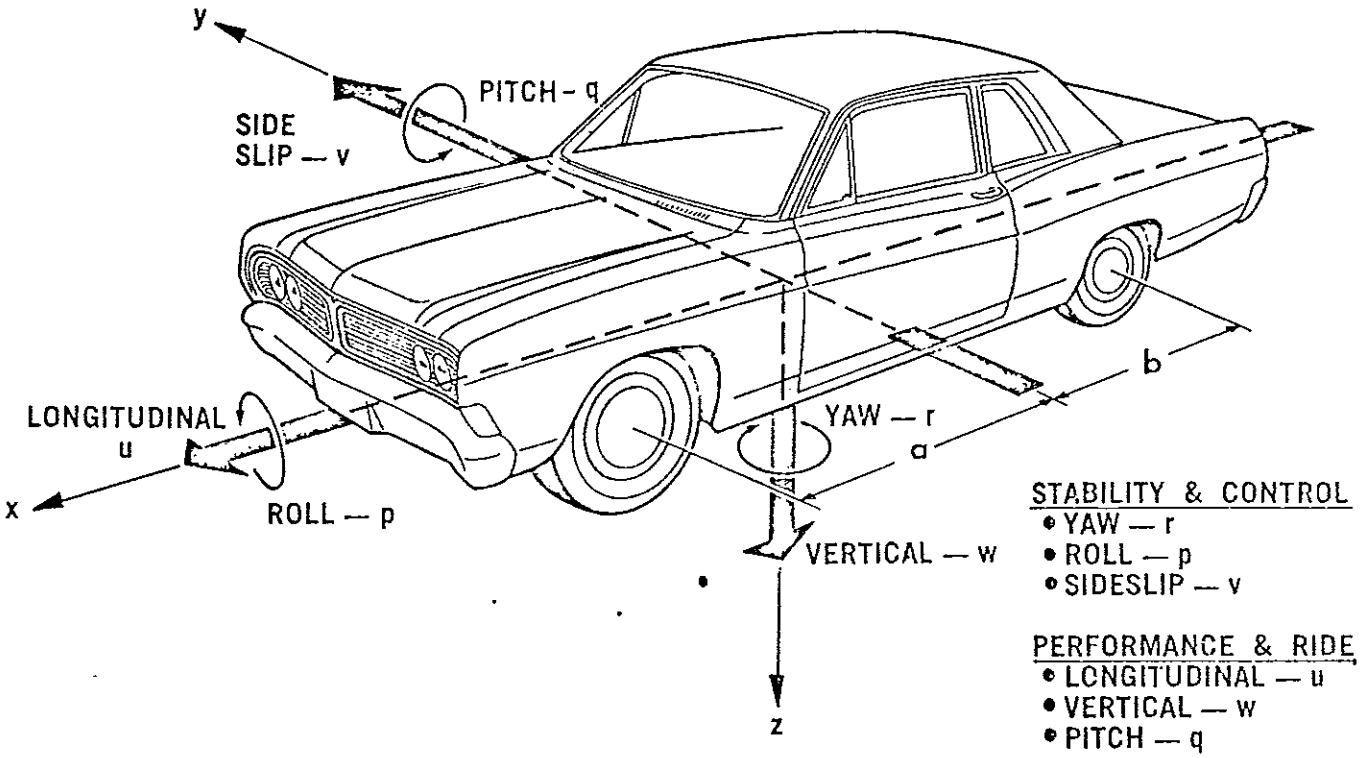

Figure 2

2 DEGREE OF FREEDOM SIMULATION
(YAW AND SIDESLIP)

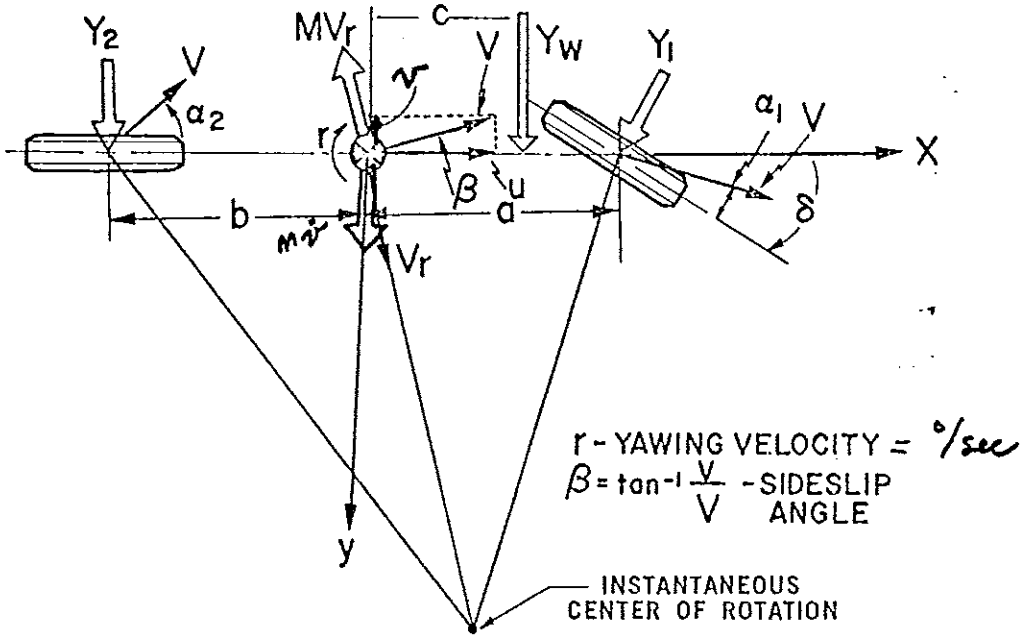

Figure 3

$$\vec{V}_{cm} = u\vec{i} - v\vec{j}$$

but $\vec{i}$ & $\vec{j}$ rotate with vehicle

$$\vec{a}_{cm} = \dot{u}\vec{i} + u\dot{\vec{i}} - \dot{v}\vec{j} - v\dot{\vec{j}} \qquad (\vec{\omega} = r\vec{k})$$

$$= \dot{u}\vec{i} + u(r\vec{k}\times\vec{i}) - \dot{v}\vec{j} - v(r\vec{k}\times\vec{j})$$

$$= (\dot{u} + vr)\vec{i} + (-\dot{v} + ur)\vec{j}$$

Inertia force

$$\vec{F} = -m\vec{a}_{cm}$$

$$= -m(\dot{u} + vr)\vec{i} + m(\dot{v} - ur)\vec{j}$$

one force (sideslip) and one moment (yaw). The inertial forces and moments are derived from Newton's basic laws of motion. The details of this derivation are too complex and lengthy for presentation here but an excellent treatment is given in Reference 5.

Because the vehicle yaws while traveling at a constant forward speed, it develops a centrifugal force equal to MVr acting along a line perpendicular to the resultant velocity of the c.g. of the vehicle. The angle that the resultant velocity makes with the x axis is called the sideslip angle, β. Because this angle is small, it can be assumed that the centrifugal force MVr acts along the y axis. Also acting along the y axis is an inertial force, $M\dot{v}$, due to the rate of change of sideslip velocity, v. The total inertial force along the y axis, then, is the sum of these two components.

The external forces acting on the vehicle along the y axis are developed by the tires and a side force due to a cross wind force acting at the center of pressure of the vehicle. It is assumed that the front wheel steer angle, δ, is small, then the sideslip equation of equilibrium is defined in equation 1.

For the yaw equation of equilibrium about the vertical z axis, the inertial moment is the product of the moment of inertia and the angular acceleration about the z axis. The external yaw moments are obtained by simply summing moments about the z axis due to the tire and wind forces, thus completing the second equation of equilibrium (equation 2).

EQUATIONS OF EQUILIBRIUM:

Sideslip

$$M(Vr \oplus \dot{v}) = Y_1 + Y_2 + Y_w \tag{1}$$

Yaw

$$I_z \dot{r} = aY_1 - bY_2 + cY_w \tag{2}$$

The next step is to define the tire forces in terms of the motion variables. Experimental investigations have shown that for given vertical loads the cornering force varies with the tire slip angle as shown in Figure 4. The slip angle is the angle between the plane of the tire and its velocity vector. For small slip angles and moderate changes in vertical load, the cornering force is assumed to be directly proportional to the slip angle, resulting in equations (3) and (4).

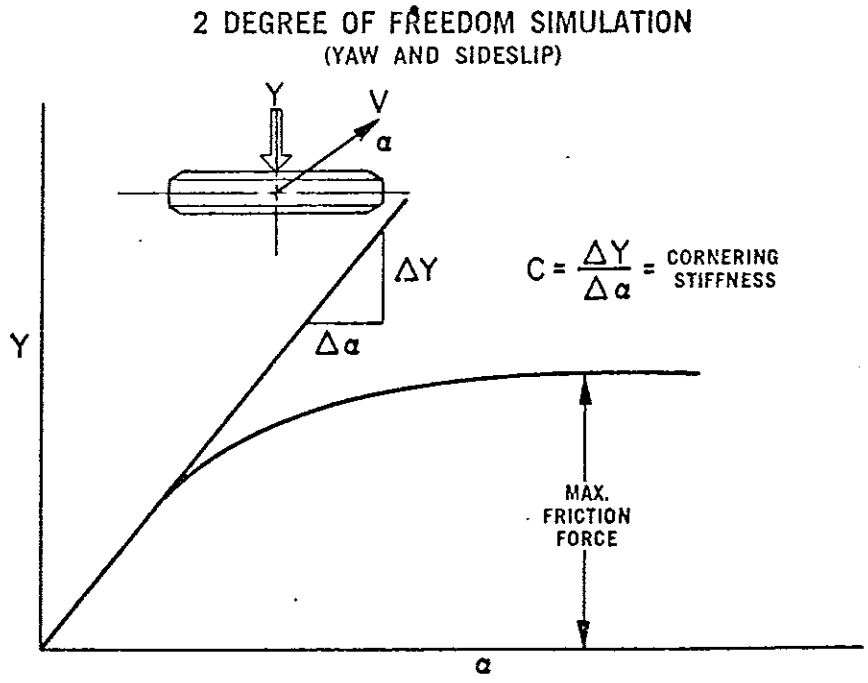

Figure 4

TIRE FORCE EQUATIONS

$$Y_1 = C_1 \alpha_1 \tag{3}$$

$$Y_2 = C_2 \alpha_2 \tag{4}$$

To complete the tire force equations, it is necessary to relate the tire slip angles to the motion variables of the vehicle. The slip angle is defined as the lateral velocity of the plane of the tire divided by the forward velocity in the plane of the tire. Because of small angles and because the forward velocity is assumed constant, the lateral velocity at each end of the vehicle is the lateral velocity of the c.g. of the vehicle, v, plus the lateral velocity at each end of the vehicle relative to the c.g. For the front, the lateral velocity relative to the c.g. is the product, ar. Summing this velocity, with the lateral velocity of the c.g. and dividing by the forward velocity, V, of the vehicle gives the first term in equation (5). This term represents the angle between the x axis of the vehicle and the front velocity vector, which is the sideslip angle of the front of the vehicle. The tire slip angle, however, is the angle between the velocity vector and the plane of the wheel, which is the difference between the front vehicle sideslip angle and the front wheel steer angle, completing equation (5).

Similarly, the rear tire slip angle is the difference of the lateral velocity of the c.g., v, and the lateral velocity of the rear of the vehicle relative to the c.g., br, divided by the forward velocity, resulting in equation (6).

2 DEGREE OF FREEDOM SIMULATION
(YAW AND SIDESLIP)

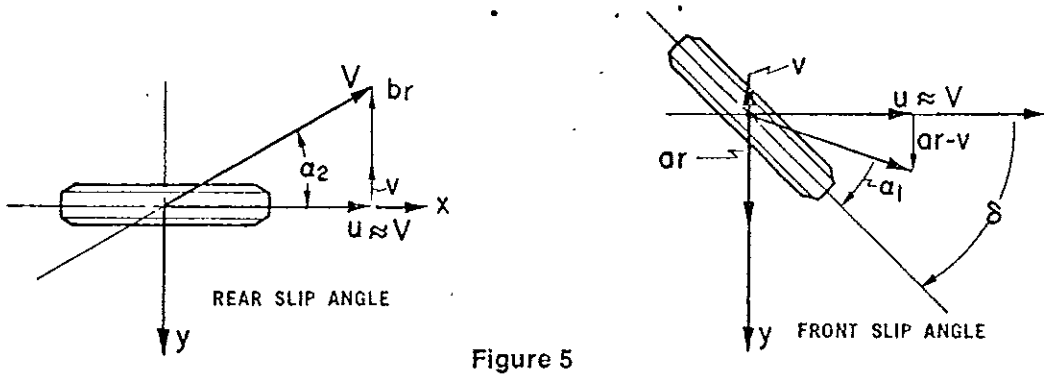

Figure 5

SLIP ANGLE EQUATIONS

$$\alpha_1 = \frac{v + ar}{V} + \delta \tag{5}$$

$$\alpha_2 = \frac{v + br}{V} \tag{6}$$

Combining the slip angle equations, tire force equations, and the equations of equilibrium, and using operator notation results in two linear simultaneous differential equations, in terms of the yawing velocity, r, and the sideslip velocity, v, which are the dependent variables, and the front wheel steer angle, δ, and the cross wind side force, Y_w, which represent arbitrary input functions.

FINAL EQUATIONS OF MOTION

$$\left[MV + \frac{1}{V}(C_1 a - C_2 b)\right] r + \left[MS + \frac{1}{V}(C_1 + C_2)\right] v = C_1 \delta + Y_w \tag{7}$$

$$\left[I_z S + \frac{1}{V}(C_1 a^2 + C_2 b^2)\right] r + \left[\frac{1}{V}(C_1 a - C_2 b)\right] v = C_1 a \delta + c Y_w \tag{8}$$

$S = Sec^{-1}$

These differential equations represent the final equations of motion for a 2 degree of freedom simulation. For systems greater than 2 degrees of freedom, the procedure is essentially the same, except each degree of freedom adds an additional equation to the final system of differential equations.

SOLUTION OF THE EQUATIONS OF MOTION

For the case of dynamic systems, it is usually desired to observe the response or output of a given system to some type of input. A mathematically convenient type of input that is used is the step function, which for the present simulation could be a step steering wheel angle input, as shown in Figure 6.

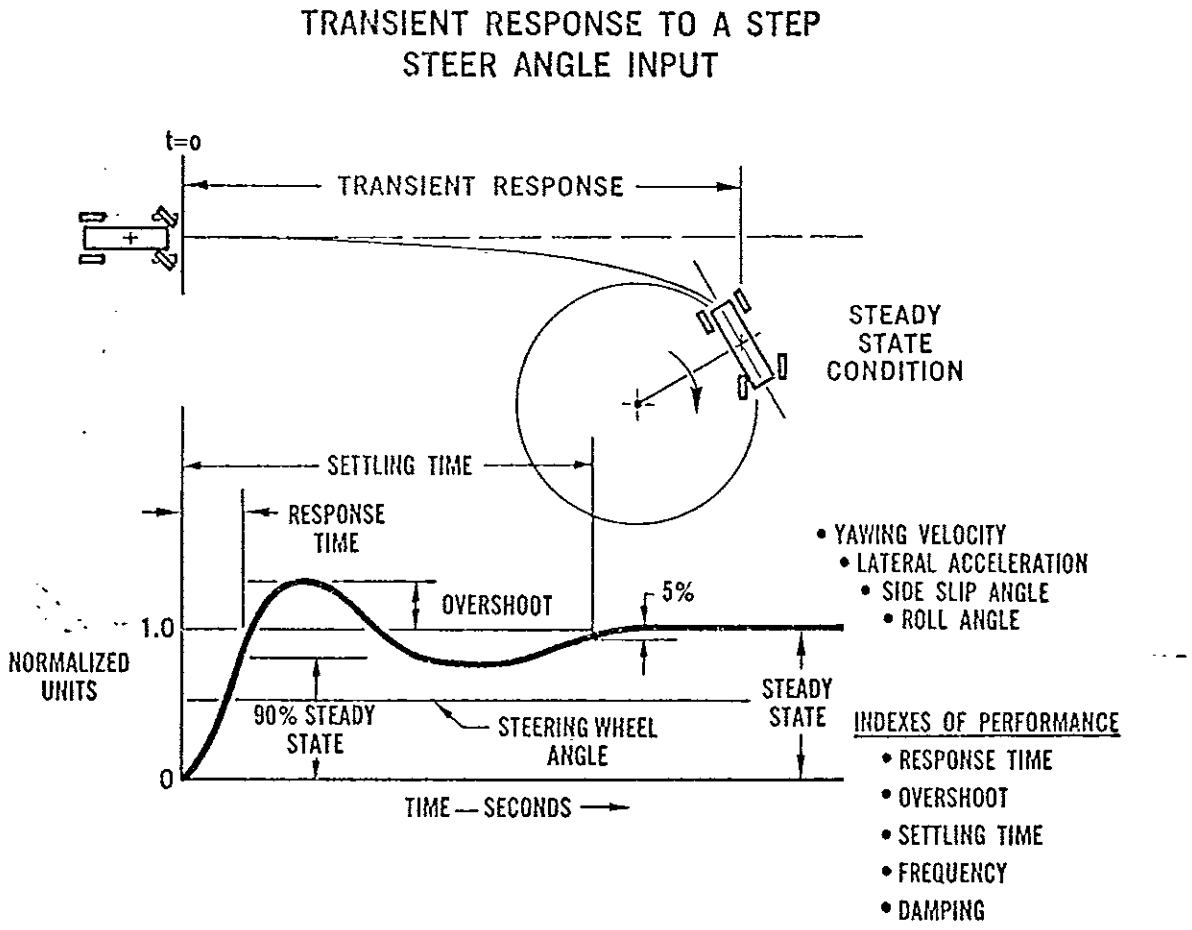

Figure 6

The output or response resulting from such an input consists of a transient part and a steady state part. That part that varies with time is called the transient. The response resulting after the transient dies out is called the "steady state" response, which is time-invariant. For the present simulation, the output could be either the yawing velocity or the sideslip velocity.

The steady state response reveals the magnitude of the motion that will be achieved for a given magnitude of input. The transient portion of the response curve tells the manner in which this magnitude is achieved. Experience has shown that certain information obtained from the transient response curve are useful indexes of system performance, as shown in Figure 6. Taking a ratio of the output steady state response magnitude to the input is also a useful steady state index of performance, commonly referred to as the "gain" of a system. This index gives a measure of the sensitivity of the specific motion variable to the given input.

In any case, both steady state and transient response characteristics are required to adequately define dynamic system response.

If the equations are linear simultaneous differential equations with constant coefficients, it is possible to obtain explicit algebraic closed form solutions for the transient and steady state response. However, if more than 2 or 3 degrees of freedom are simulated, the resulting equations are too complicated to be useful for analysis. Solutions with digital and hybrid analog computers are usually used for complex systems, especially when system non-linearities are considered.

STEADY STATE RESPONSE

Analysis has shown that various steady state solutions yield important algebraic relations that are useful as steady state performance indexes. These solutions, which will be described next, were derived from a 3 degree of freedom vehicle simulation (yaw, roll, and sideslip) plus 2 degrees of freedom of the steering system (steering wheel rotation and the combined front wheel steering motion). The equations of motion for this simulation are developed in detail in Reference 7.

Understeer

Solution of the equations of motion in terms of the steering wheel angle gives:

$$\theta_{sw} = n\left[\frac{\ell}{R} + U\left(\frac{V^2}{R}\right)\right] \tag{9}$$

For the case where the radius, R, is held constant, the required steering wheel angle is directly proportional to the lateral or centripetal acceleration. Figure 7 graphically displays this condition.

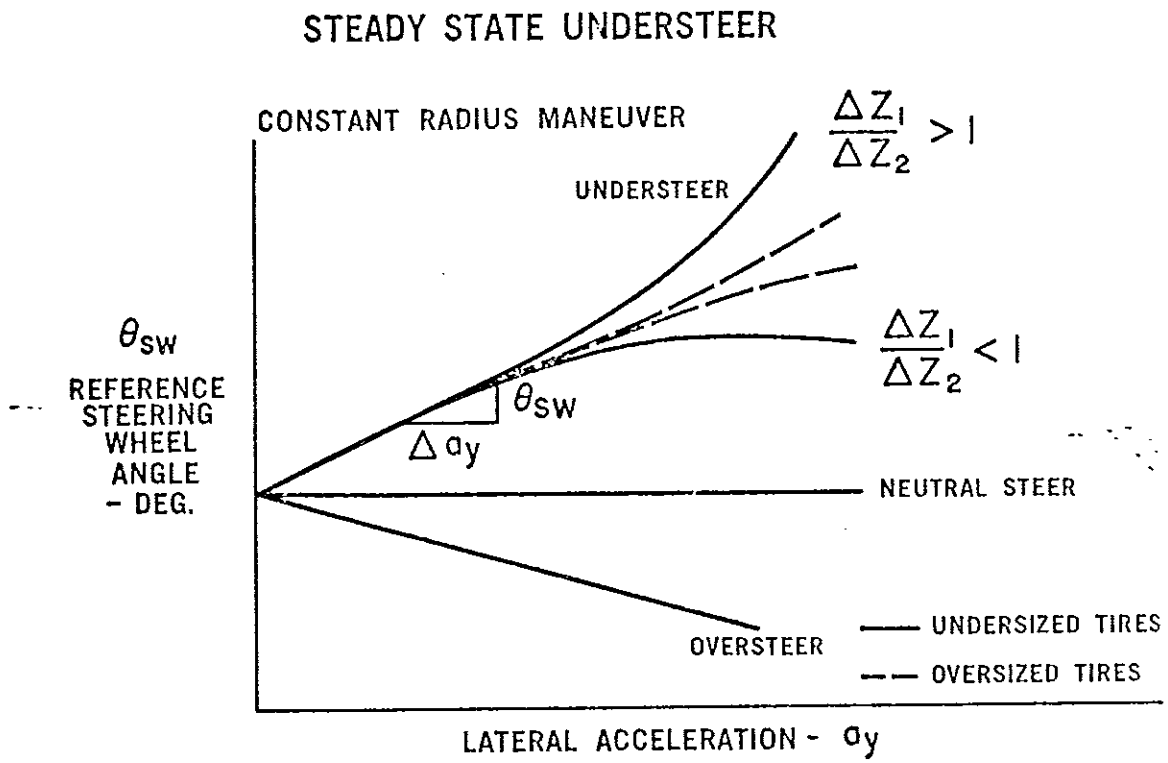

Figure 7

Zero speed or zero lateral acceleration defines the Ackerman steering wheel angle. The change in required steering wheel angle is dependent on the magnitude and sign of the understeer coefficient, U. When U is positive, an increase in steering wheel angle is required and the vehicle is said to be "understeered." If U is zero, no change in steer angle is required and the vehicle is said to be "neutral steered." A negative value for U requires a decreasing steer angle, which defines an "oversteered" vehicle.

Analysis with mathematical models that provide for nonlinear tire characteristics show that the lateral load transfer distribution, $\Delta Z_1 / \Delta Z_2$, is an important index of performance in defining the understeer of a vehicle during high g cornering. A cornering vehicle transfers load from the inside wheels to the outside wheels (Figure 12). The radio of this load transfer at the front to the load transfer at the rear is defined as the load transfer distribution, $\Delta Z_1 / \Delta Z_2$. An equation for computing this ratio is described in a succeeding section.

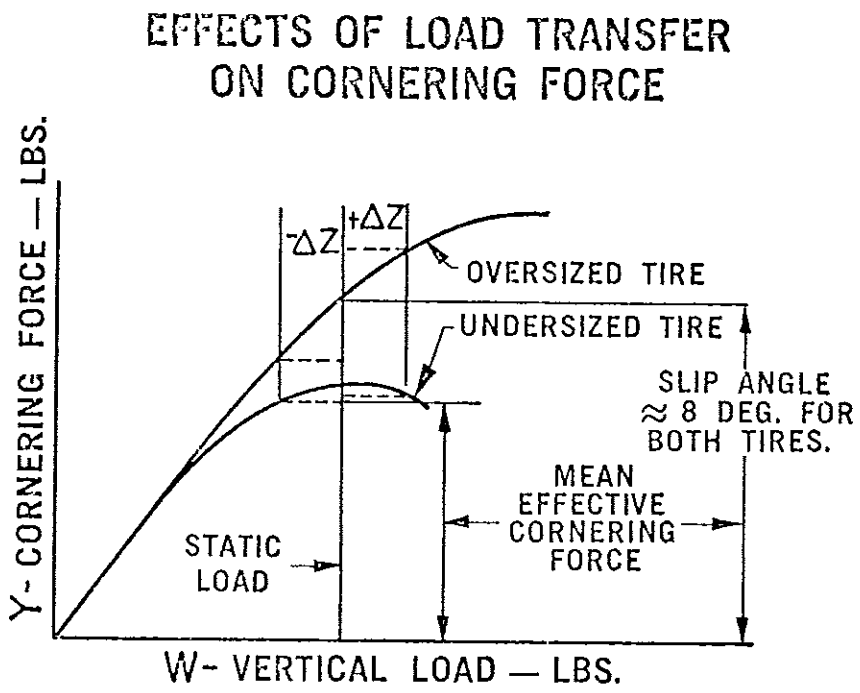

Figure 8

When $\Delta Z_1 / \Delta Z_2 < 1.0$, a vehicle that is understeered at the lower lateral accelerations can reverse into an oversteering vehicle. A vehicle having this characteristic will tend to spin out under hard cornering conditions.

The effect of $\Delta Z_1 / \Delta Z_2$ on the understeer is explained in Figure 8.

Shown is a cornering force vs vertical load curve for a high slip angle condition. Representative curves for two different size tires are presented. It is assumed that these tires are applied to the same vehicle which has the indicated static load.

When a vehicle corners, weight is transferred from the inside to the outside wheel. This transfer of load is designated by ΔZ in Figure 8. For the so-called undersized tire, both the inside and outside wheel experience a reduction in cornering force. Thus, in order to maintain the same total cornering force, an increase in slip angle must occur. In the case of the oversized tire, the cornering force of the outside tire increases by almost the same amount that the inside tire decreases, thus maintaining the same total cornering force with no required change in slip angle.

Thus a vehicle that is equipped with undersized tires will be very sensitive to the $\Delta Z_1 / \Delta Z_2$ ratio. If more load transfer is taken by the front wheels, $\Delta Z_1 / \Delta Z_2 > 1.0$ larger front slip angles will be required and the understeer increases. Conversely, when $\Delta Z_1 / \Delta Z_2 < 1.0$ larger rear slip angles are required and the vehicle becomes oversteered.

For a vehicle equipped with oversized tires, such as race cars, the $\Delta Z_1 / \Delta Z_2$ has a minor effect on the understeer as shown in Figure 7.

In summary, the required steering wheel angle for a given constant radius maneuver is primarily dependent on the overall steering ratio, the wheelbase, the understeer coefficient U, and the load transfer ratio, $\Delta Z_1 / \Delta Z_2$. The overall steering ratio and wheelbase are single parameters that can be altered individually. The understeer coefficient U, and the load transfer ratio, $\Delta Z_1 / \Delta Z_2$, however, are dependent on a combination of several design parameters of a vehicle. The understeer coefficient, U, is the basic parameter used in defining the yaw velocity, lateral acceleration, and sideslip angle gains, which will be described in succeeding sections. U is usually expressed in units of deg./g. Because of the basic importance of the understeer coefficient, the equation for computing its value is described in detail in the next section.

The coefficient, U, is an algebraic expression in terms of the tire, vehicle, and steering system parameters only. Its total value is computed from the sum of the following components:

UNDERSTEER COMPONENT	DUE TO THE EFFECTS OF:
$U = \frac{W_1}{2C_1} - \frac{W_2}{2C_2}$	Weight distribution and tire cornering stiffness
$+\left(\frac{S_1}{C_1}\frac{d\gamma_1}{d\phi} - \frac{S_2}{C_2}\frac{d\gamma_2}{d\phi}\right)\frac{d\phi}{da_y}$	Suspension roll camber and tire camber stiffness
$+\left(\epsilon_1 + \epsilon_2\right)\frac{d\phi}{da_y}$	Suspension roll steer
$+ W_{s1} A_1 + W_{s2} A_2$	Lateral suspension compliance steer
$+ \frac{W_1 K_{ss}}{12}\left(\frac{AT_1}{C_1} + \xi R_w\right)$	Steering compliance
$+ \frac{AT_1 + AT_2}{C_1 C_2 \ell 2}\left[W + 2\left(S_1\frac{d\gamma_1}{d\phi} + S_2\frac{d\gamma_2}{d\phi}\right)\frac{d\phi}{da_y}\right]$	Tire alignment torque (total vehicle)
$+ \frac{\partial X}{\partial Z}\frac{RR}{\ell}\left(\frac{1}{C_1} + \frac{1}{C_2}\right)\sum_{1,2} t\,\frac{\Delta Z}{\Delta a_y}$	Tire rolling resistance

Equation 10

The first component reflects the effects of weight distribution and tire cornering stiffness. This term results from the 2 degree of freedom simulation that was developed in this paper. This component is a basic design parameter for all vehicles and is very useful in evaluating the effects of various types and sizes of tires for a given vehicle. As an aid for determining the value of this component, a plot of tire cornering data shown in Figure 9 is useful.

This curve is constructed from tire data by plotting the ratio of vertical load to cornering stiffness versus the vertical load. Representative data for a bias ply and a radial ply tire are shown. If it is assumed that a given vehicle has front and rear wheel loads designated by "A" and "B" respectively (front heavy) then the understeer for each type of tire can readily be determined from the curves as shown. The bias ply tire produces a significantly greater amount of understeer than the radial ply tire (1.10 deg./g. vs 0.40). If the weight distribution were reversed, where "B" would now be the front load and "A" the rear load, then the same values of understeer would become oversteer.

The difference between the bias ply and radial ply curves is similar to differences produced by changes in tire pressures. The bias ply being similar to lower pressures and the radial ply being similar to higher pressures for the same tire.

As shown, presentation of tire cornering stiffness data in this manner gives a very simple and effective method for assessing the influence on understeer of various types of tires, tire sizes, pressures, vehicle loading, and changes in vehicle loading due to passengers and baggage.

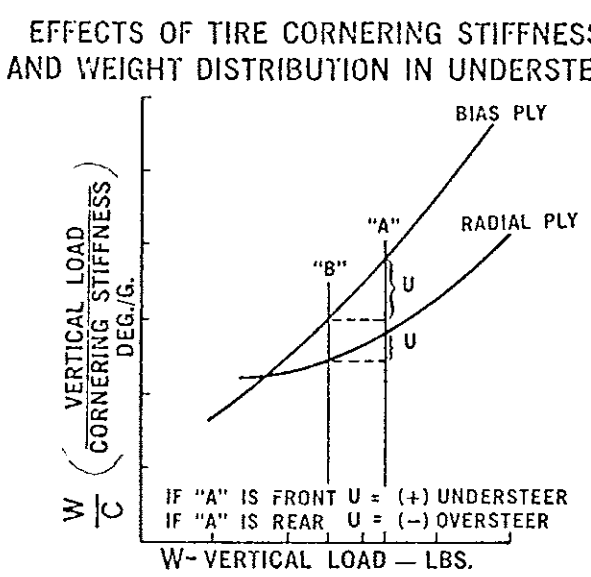

Figure 9

The next term, from equation 10, gives primarily a measure of the effects of suspension roll camber, vehicle roll flexibility, and the ratio of camber stiffness to cornering stiffness on the understeer coefficient of the vehicle. The roll camber $d\gamma/d\phi$, is the rate of change of camber angle per unit change in vehicle roll angle and is a function of the suspension geometry. This factor can be computed simply from a standard camber change curve.

Vehicle roll flexibility, $d\phi/da_y$, is defined as the rate of change of roll angle per unit change in lateral acceleration. Analysis and experiment have shown that this value is a constant for a vehicle with approximately linear spring rates (Figure 14). The equation for computing this value is described in a succeeding section.

Tire camber stiffness, as shown in Figure 10, is a measure of the change in camber thrust per unit change in camber angle for a given vertical load.

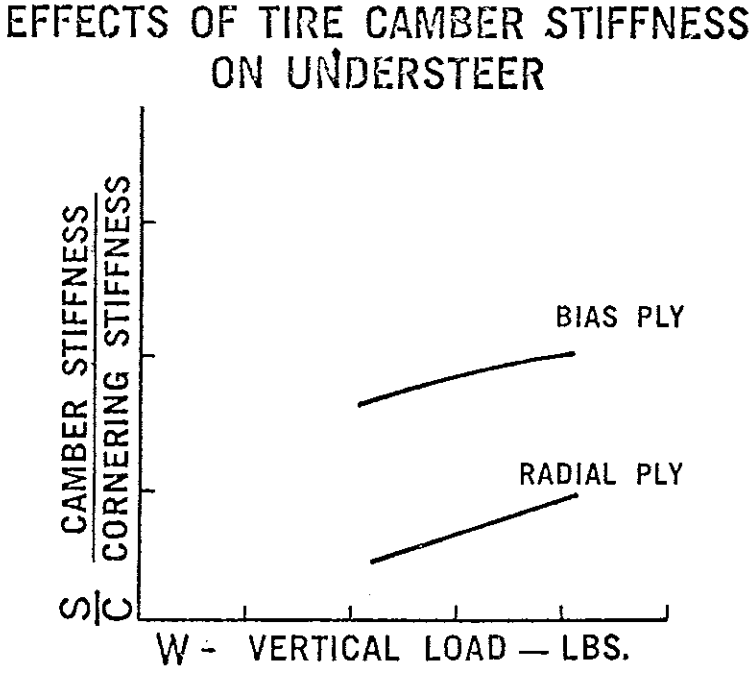

Figure 10

Also shown in Figure 10 is a graph of the ratio of camber stiffness to cornering stiffness versus vertical load for a typical bias ply and a radial ply tire. For a given vehicle that has an independent front suspension and a solid axle rear suspension with a given roll flexibility and front roll camber, the bias ply tire will contribute about 3 times more understeer than the radial ply tire.

From the discussion thus far it can be concluded that replacing bias ply tires on a typical front heavy sedan (independent front, solid axle rear) with radial ply tires will produce a significant reduction in the understeer coefficient U.

The next term in equation 10 defines the effects of roll steer, which is defined as the change in steer angle per unit change in roll angle. For an independent suspension, the roll steer results from the toe change due to vertical wheel motion.

The effect of roll steer on the understeer coefficient is directly proportional to the vehicle roll flexibility, again pointing out the importance of roll flexibility as an index of performance.

The understeer due to lateral suspension compliance steer is directly proportional to the sprung weight and the compliance steer in degrees of steer per unit of side force.

When a vehicle corners, a tire aligning torque is developed about the kingpin axis of each front wheel in a direction that opposes the angle of steer. Because of compliance between the front wheels and the steering wheel, this aligning torque will reduce the front wheel angle for a given steering wheel angle by winding up the steering system. This is an understeering effect.

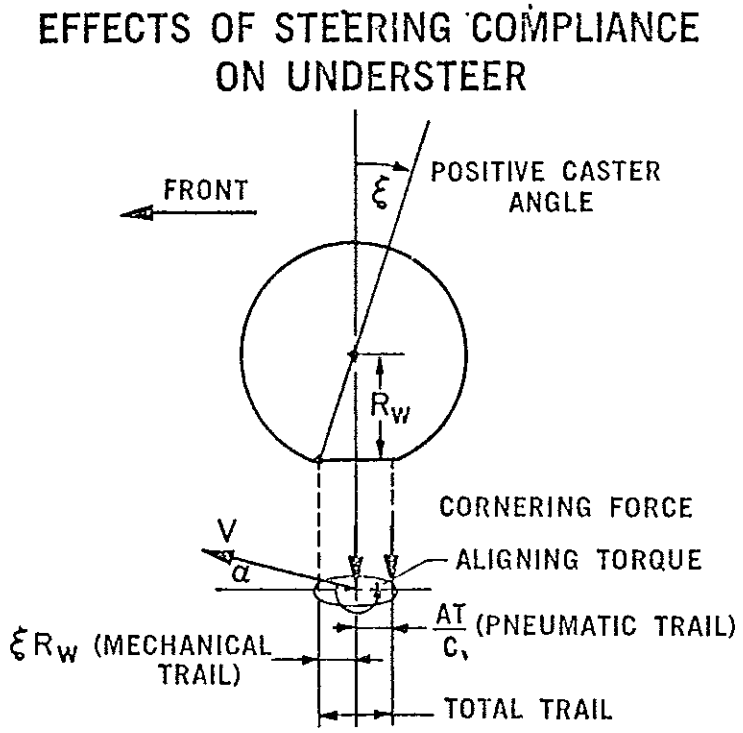

Figure 11

As illustrated in Figure 11, the term AT_1/C_1 is the ratio of the aligning torque stiffness to the cornering stiffness, which is often referred to as the "pneumatic trail." This is the offset in the ground plane between the point of application of the cornering force and a vertical axis located on the axle centerline. The term, ξR_w, is the offset between a vertical axis through the axle centerline and the intersection in the ground plane of the kingpin axis, inclined at a given caster angle. This effect is sometimes referred to as "caster offset" or "mechanical trail." For a positive caster (kingpin axis rotated to the rear) the mechanical and pneumatic trails are additive. A negative caster subtracts from the pneumatic trail.

This trail multiplied by the weight on the front wheels and the effective steering system compliance, K_{ss}, defines the value of understeer due to steering compliance. Experience has shown that this value is a sizable amount for typical American sedans.

The last two terms in equation 10 are of minor importance and define the understeer due to the torque induced on the vehicle from the tire aligning torques and the torque produced by unsymmetrical tire rolling resistance forces acting between right and left wheels due to weight transfers. These torques always oppose the turning of the vehicle and are an understeering factor.

Roll Flexibility

Solution for roll angle is of the form:

$$\frac{\Delta \phi}{\Delta a_y} = \left[\frac{W_s h_s + \sum_{1,2} W_u h_u \frac{d\gamma}{d\phi}}{K_1 + K_2 - W_s h_s - \sum_{1,2} W_u h_u \left(\frac{d\gamma}{d\phi}\right)^2} \right] \qquad (11)$$

This equation assumes fixed front and rear roll centers for defining the roll arm, h_s. The equation is also valid for either an independent or solid axle suspension. For the case of a solid axle, the roll camber, $d\gamma / d\phi$, is zero. Figures 12 and 13 describe the forces and moments acting on the sprung and unsprung masses.

FORCES AND MOMENTS ACTING ON THE SPRUNG AND UNSPRUNG MASSES

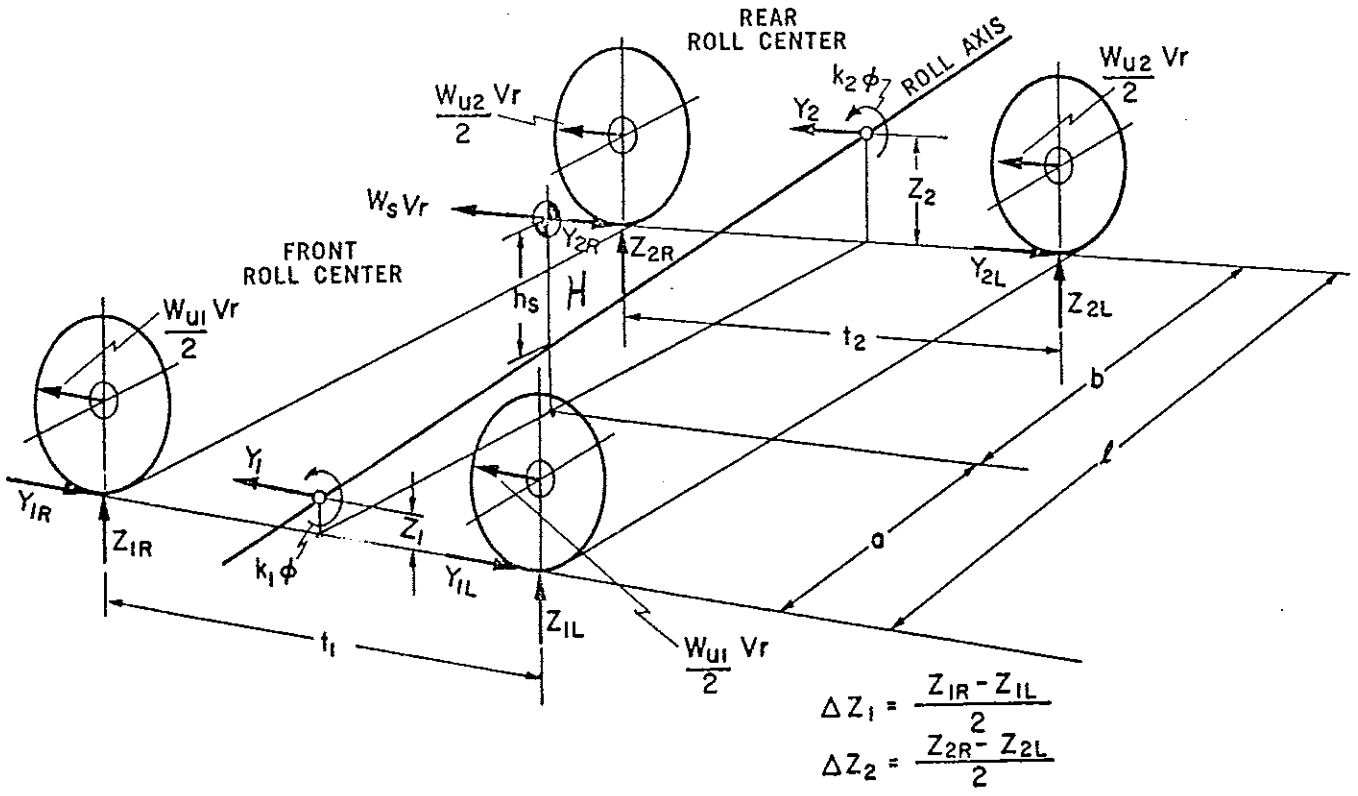

Figure 12

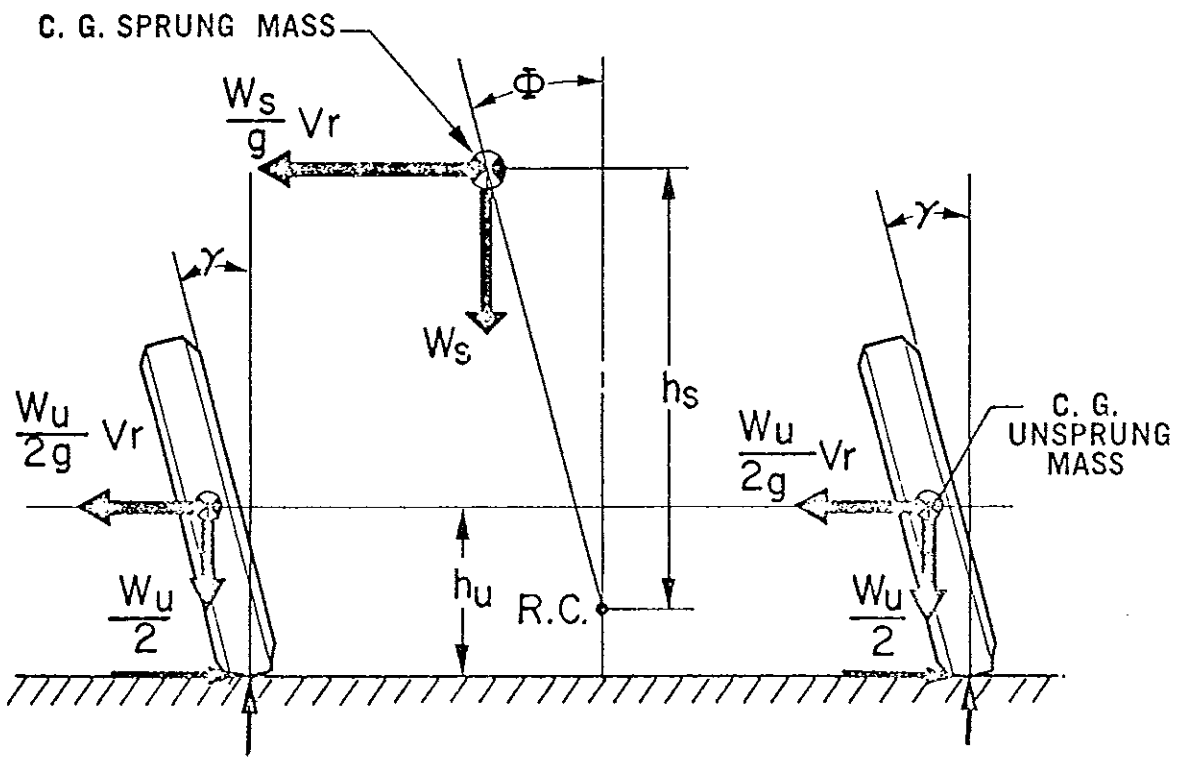

Figure 13

This equation is presented in Figure 14, which shows that the roll angle is directly proportional to the lateral acceleration for linear roll rates. The roll flexibility is defined as the slope of this curve and is a measure of the sensitivity of a vehicle to roll. Since suspension roll steer and roll camber are proportional to vehicle roll, the roll flexibility is an important performance index that determines the influence of these characteristics on vehicle understeer, as described in a preceding section.

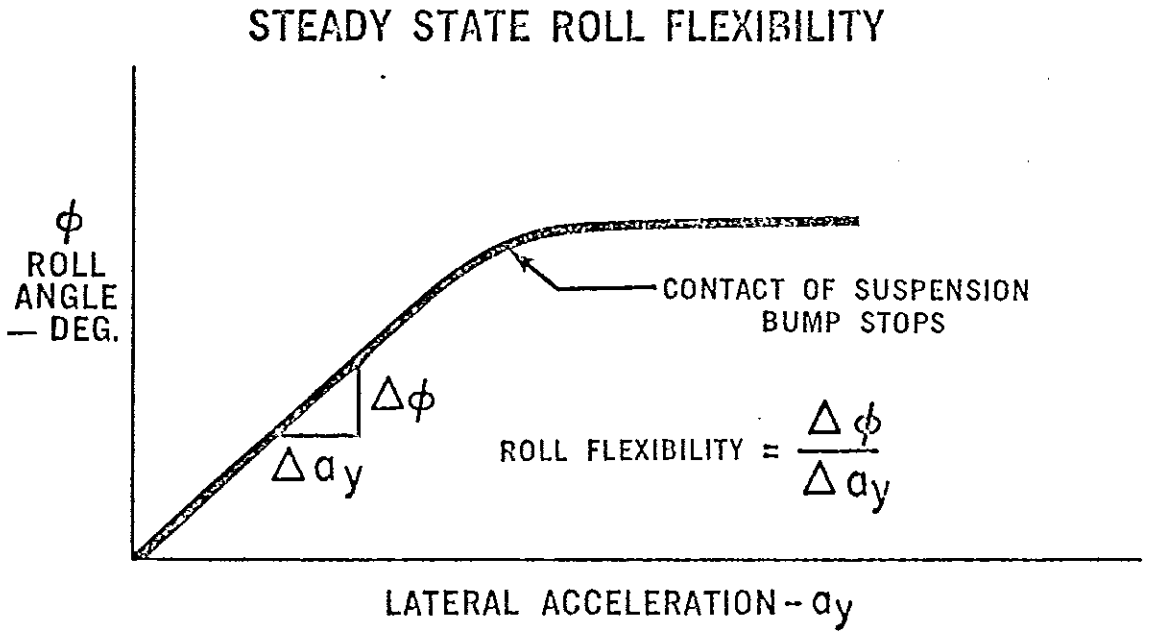

Figure 14

The accuracy of equation 11 has been checked by computing the roll angle vs. lateral acceleration curve with a six degree of freedom simulation that does not assume fixed roll centers. The correlation was excellent. The equation is simple enough for hand calculation or for programming on a time sharing computer.

Roll Couple

Load Transfer Distribution $\Delta Z_1/\Delta Z_2$

The centrifugal force of a cornering vehicle acting at a distance above the ground produces a roll couple tending to overturn the vehicle. This roll couple is reacted by front and rear roll couples produced by a transfer of load from the inside to the outside wheels. As described in a previous section, experience has shown that the ratio of the front lateral load transfer to the rear lateral load transfer, $\Delta Z_1/\Delta Z_2$, is an important index of performance for defining the understeer of a vehicle at high lateral accelerations. The solution for load transfer distribution takes the following form:

$$\frac{\Delta Z_1}{\Delta Z_2} = \frac{t_2}{t_1}\left[\frac{W_{s1}\, z_1 + W_{u1}\, h_{u1}\left(1 - \frac{d\gamma_1}{d\phi}\right) + \left\{K_1 + W_{u1}\, h_{u1}\frac{d\gamma_1}{d\phi}\left(1 - \frac{d\gamma_1}{d\phi}\right)\right\}\frac{d\phi}{da_y}}{W_{s2}\, z_2 + W_{u2}\, h_{u2}\left(1 - \frac{d\gamma_2}{d\phi}\right) + \left\{K_2 + W_{u2}\, h_{u2}\frac{d\gamma_2}{d\phi}\left(1 - \frac{d\gamma_2}{d\phi}\right)\right\}\frac{d\phi}{da_y}}\right] \qquad (12)$$

This equation defines load transfer distribution for either an independent or solid axle suspension. As in the equation for roll flexibility, the roll camber, $d\gamma/d\phi$, is zero for a solid axle suspension. Note that for the case of an independent suspension, $d\gamma/d\phi \neq 0$, the load transfer distribution is a function of the roll flexibility $d\phi/da_y$. Results computed from this equation also give excellent agreement with results from the six degree of freedom simulation. The equation is also simple enough for hand calculation or for programming on a time sharing computer.

Yawing Velocity Gain

Solution of the equations of motion for a 3 degree of freedom vehicle simulation, plus a degree of freedom representing the combined effect of the front wheels about a steering axis in the plane of the wheel, yields the following expression for yawing velocity.

$$\frac{r}{\theta_{sw}} = \frac{V}{n\,(\ell + U\,V^2)} \qquad (13)$$

Equation 13 is illustrated in Figure 15. For the case of U = O (neutral steer) the yaw gain is directly proportional to speed. When U > O , the yaw gain is less than for a neutral-steered vehicle and the vehicle is said to

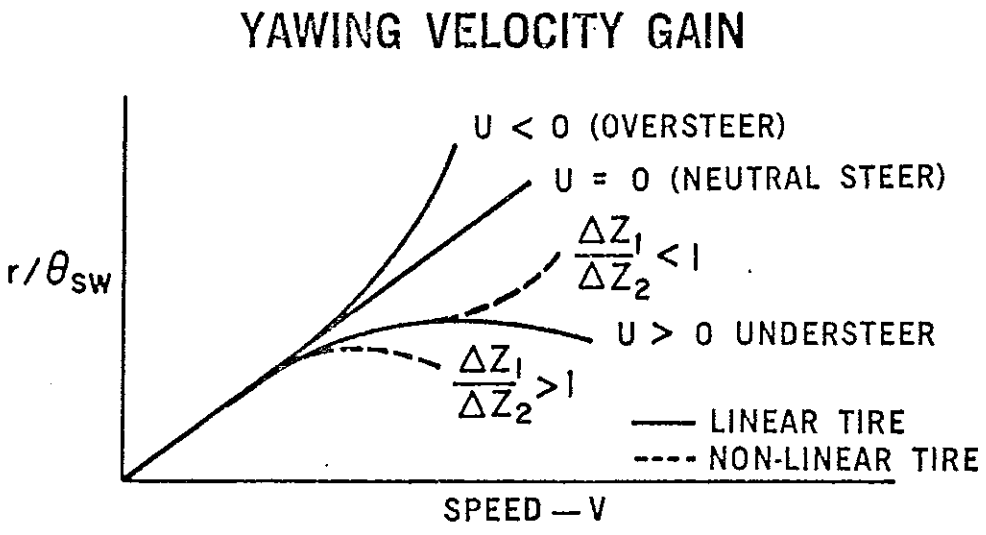

Figure 15

understeer. If $U < 0$, the yaw gain is greater than that of a neutral-steered vehicle and the vehicle is said to oversteer. At some finite speed, the gain of an oversteering car is infinite, indicating an unstable condition. This speed is defined as follows:

$$V_{cr} = \sqrt{\frac{\ell}{U}} \tag{14}$$

Experience has shown that it is very unlikely for a conventional vehicle to be oversteered at low lateral accelerations.

The dashed curves in Figure 15 illustrate the effects of load transfer distribution, $\Delta Z_1/\Delta Z_2$ on the yaw gain of an understeered vehicle at high trim (lateral acceleration) conditions. When $\Delta Z_1/\Delta Z_2 > 1.0$ the yaw gain at the higher speeds is reduced, and conversely, when $\Delta Z_1/\Delta Z_2 < 1.0$, the yaw gain will increase at the higher speeds and assume an oversteering characteristic.

Lateral Acceleration Gain

The lateral acceleration gain is obtained by multiplying the yawing velocity gain by the speed, V.

$$\frac{Vr}{\theta_{sw}} = \left[\frac{V^2}{n(\ell + U V^2)}\right] = \frac{1}{n\left(\frac{\ell}{V^2} + U\right)} = \frac{100}{n\left[\left(\frac{(\ell/12) \times g \times 180}{V^2 \pi}\right) + U\right]} \tag{15}$$

ℓ - inches

V - ft/sec

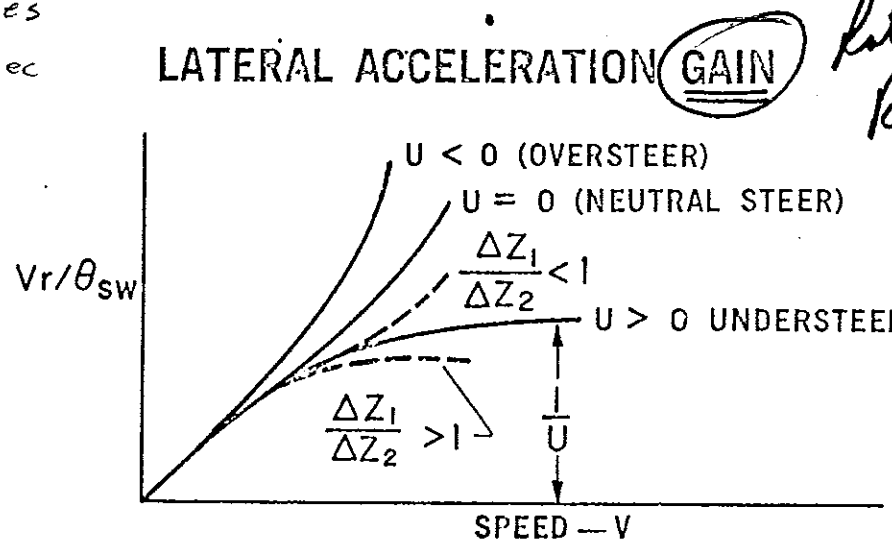

Figure 16

Equation 15 is graphically displayed in Figure 16 for an over-, neutral- and understeered vehicle. As shown, the gain of the understeered vehicle approaches the inverse of the understeer coefficient, U. Examination of equation 15 shows that the gain can be changed by changing either the overall steer ratio, n, or the understeer coefficient, U. Also shown on the graph are typical effects of tire non-linearities due to different load transfer distributions. As for the yaw gain, these non-linear gain effects, are present only when the vehicle is operating at a high trim (lateral acceleration) condition. For straight ahead driving, the gain is represented by equation 15 and the linear tire curve. The gain of the oversteer vehicle becomes infinite at the same critical speed as does the yawing velocity gain (equation 14).

Sideslip Angle Gain

Solution of the equations of motion for the sideslip angle yields the following:

$$\frac{\beta}{\theta_{sw}} = \frac{b + U_2 V^2}{n(\ell + U V^2)} \tag{16}$$

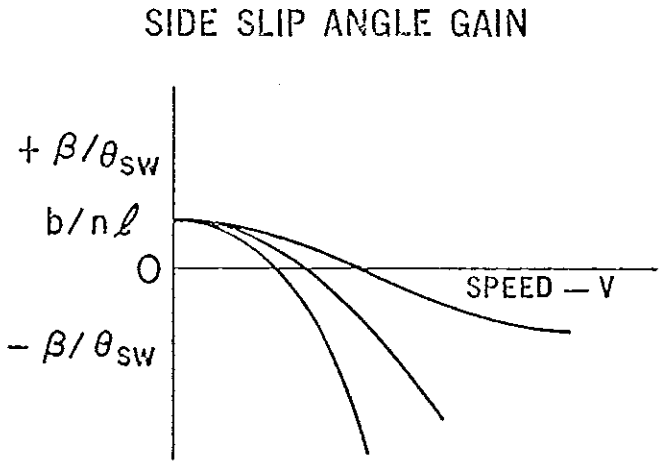

Figure 17

Figure 17 shows a graphical display of the sideslip angle gain as a function of increasing speed for an over-, neutral- and understeer vehicle. Note that all vehicles start out at the same positive value, equal to b/nℓ and then pass through zero and become negative. As did the yawing velocity and the lateral acceleration gain, the sideslip gain of the oversteered vehicle becomes infinite at the same critical speed.

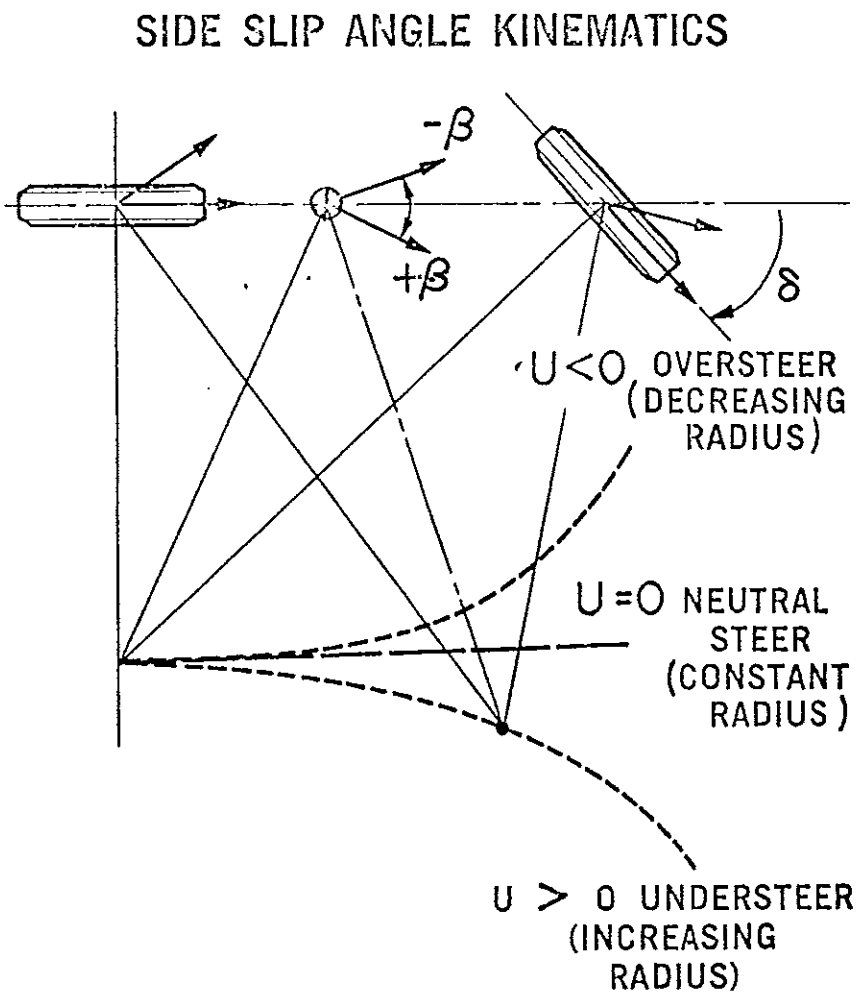

Figure 18

Figure 18 pictorially describes the kinematics of equation 16 and Figure 17. At zero speed the sideslip angle is positive and the tire slip angles are zero since no tire forces are required. This radius is called the Ackerman radius. As the vehicle speed increases, the centrifugal force of the vehicle must be balanced by tire forces, causing the instant center of rotation to move forward so that tire slip angles are developed. As shown, the instant center of the oversteer vehicle follows a path of decreasing radius, and the understeer has an increasing radius. However, in all cases the sideslip angle goes from a positive to negative value. As indicated in Figure 17 the sideslip angle of the understeer vehicle approached a maximum value, which is defined by:

$$\left(\frac{\beta}{\theta_{sw}}\right)_{max} = \frac{U_2}{n\,U} \tag{17}$$

Steering Wheel Torque Gradient

The cornering forces and aligning torques developed by the front tires of a cornering vehicle produce a steering torque about the kingpin axis that is reacted by the application of a torque on the steering wheel. Solution of the equations of motion for the steering wheel torque yields the following:

$$\frac{T_{sw}}{a_y} = \frac{W_1}{n}\left(\frac{AT_1}{C_1} + \xi R_w\right) \tag{18}$$

As illustrated in Figure 11, the term, AT/C is the pneumatic trail and the term ξR_w is the caster offset or the mechanical trail. The weight on the front wheels, times the total trail, defines the torque about the kingpin axis per g of lateral acceleration. Dividing by the overall steer ratio, n, defines the torque at the steering wheel per g lateral acceleration and is termed the "steering wheel torque gradient."

Figure 19 illustrates the steering wheel torque vs lateral acceleration curve for a typical vehicle.

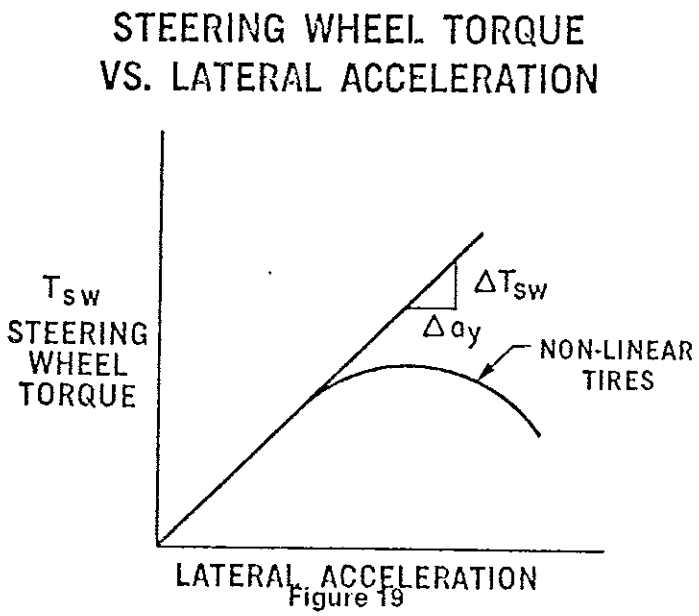

Figure 19

As shown, the torque rises to a maximum value and then decreases. This non-linearity reflects a typical aligning torque vs slip angle curve of a tire. Equation 18 defines the slope of the linear portion of the curve and is a measure of the returnability or self-centering property of the steering system. The derivation of equation 18 is given in Reference 7.

In actual practice, an experimental curve (Figure 19) would show a hysteresis loop which represents the friction in the steering system. The magnitude of this hysteresis loop is important since it magnifies the torque required on the steering wheel for a given lateral acceleration, and, because it opposes rotation, it will limit the returnability of the steering wheel and cause a dead zone which is related to the precision of steering for small steering corrections.

TRANSIENT RESPONSE

Excellent treatments of the mathematical solution for the transient response characteristics of a 2-degree and 3-degree of freedom simulation are given in References 8 and 9 respectively. The details of these derivations will not be treated here. However, formulae resulting from these derivations are very useful in describing the effects of certain design parameters on the vehicle yaw damping, response time, and natural frequency in yaw.

Equation 19, taken from Reference 9, defines an approximate relation for the damping ratio of the vehicle in yaw.

$$\zeta = \frac{1}{\sqrt{1 + \dfrac{4\ C_1 C_2\ U\ V^2}{(C_1 + C_2)^2\ \ell}}} \tag{19}$$

As shown, in Figure 20, the damping will decrease with an increase of speed or understeer coefficient, U. Damping will increase with increases in wheelbase, ℓ, or total tire cornering stiffness, $C_1 + C_2$ if $U > 0$.

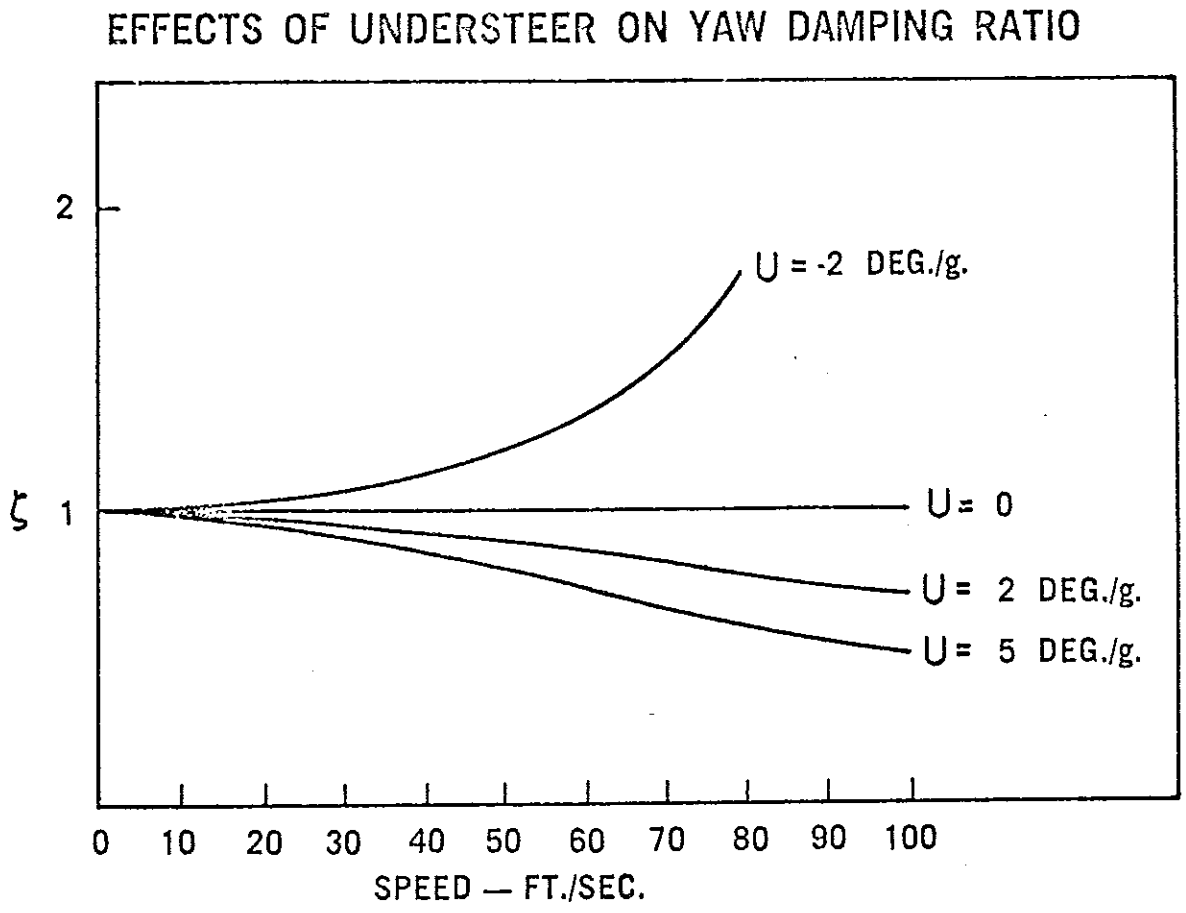

Figure 20

From the same reference, the undamped natural frequency in yaw is defined by the following approximate relation.

$$\omega_n = \sqrt{C_1 C_2\ \ell \left(U + \frac{\ell}{V^2}\right)} \tag{20}$$

The natural frequency will increase with understeer but decrease with increases of speed and moment of inertia. The damped frequency of yaw oscillation is defined by:

$$\omega_d = \sqrt{1 - \zeta^2} \tag{21}$$

As the yaw damping decreases with increased speed, the damped frequency approaches the undamped frequency. The damped frequency represents the actual frequency at which the vehicle will oscillate and changes very little with speed.

Response Time

The response time has arbitrarily been defined as the time required for a given variable of motion to reach 90 per cent of its steady state value for a given step input (Figure 6). From Reference 9, an approximate equation defines response time for a 2-degree of freedom simulation (no roll) as:

Side Slip

$$t \cong \frac{2MV}{C_1 + C_2} \left(\frac{k^2/ab}{1 + k^2/ab} \right) \tag{22}$$

This response time is defined as the time it takes to reach 1/e of its steady state value, which is different from the definition used in this paper, but the equation still reflects the effects of the given design parameters. Increases in speed and k^2/ab will increase the response time. Conversely, increases in total tire cornering stiffness and wheelbase (decreases k^2/ab) will decrease the response time. The response time computed from this equation does not reflect the effects of roll. Understeer effects due to roll (roll steer, roll camber) reduce the yawing velocity response times to a fraction of the value computed in equation 22, which more nearly reflects the value of the lateral acceleration or sideslip angle response times.

APPLICATION OF PREDICTION TECHNIQUES

Figure 21, illustrates the relation of prediction techniques to the design and development process of the vehicle.

In the planning of a new product or model year, inputs from engineering, product planning, sales, marketing, styling, and manufacturing are resolved into product objectives. These product objectives provide the basis from which design specifications are established for all aspects of the vehicle. For the case of handling, the important design parameters are the mass and inertia characteristics, the suspension and steering system, tires, and aerodynamic properties. Once the initial body package is established, the mass and inertia properties and the aerodynamics are fixed. There is room, however, for variations in suspension, steering, and tire characteristics.

The type of vehicle defined by the product objectives, determines the initial specifications for suspension, steering, and tires. From these design specifications, computations of response characteristics are made and analyzed to see whether predicted responses meet the desired performance specifications. If not, changes in the design can be made until the performance specifications are met. Because design changes may be required, it is very important that the handling analysis be conducted in the early stages of design before major hardpoints are fixed.

With the conclusion of design analysis, prototypes are built and evaluated by development engineers from which the final tuning of the vehicle will be made. Even at this late stage, if changes are required, the mathematical model can be useful in indicating changes that would help accomplish the desired performance objective.

As the mathematical model is more extensively applied in both the design and development phases, experience with the various "numbers" generated will supplement the subjective experience of development engineers and provide a basis for establishing sound performance specifications, which provide management an improved basis for decision making.

The use of prediction techniques in the development of design specifications will be treated in more detail in the next section. Following this will be a description of the use of prediction techniques to solve specific problems.

APPLICATION OF PREDICTION TECHNIQUES

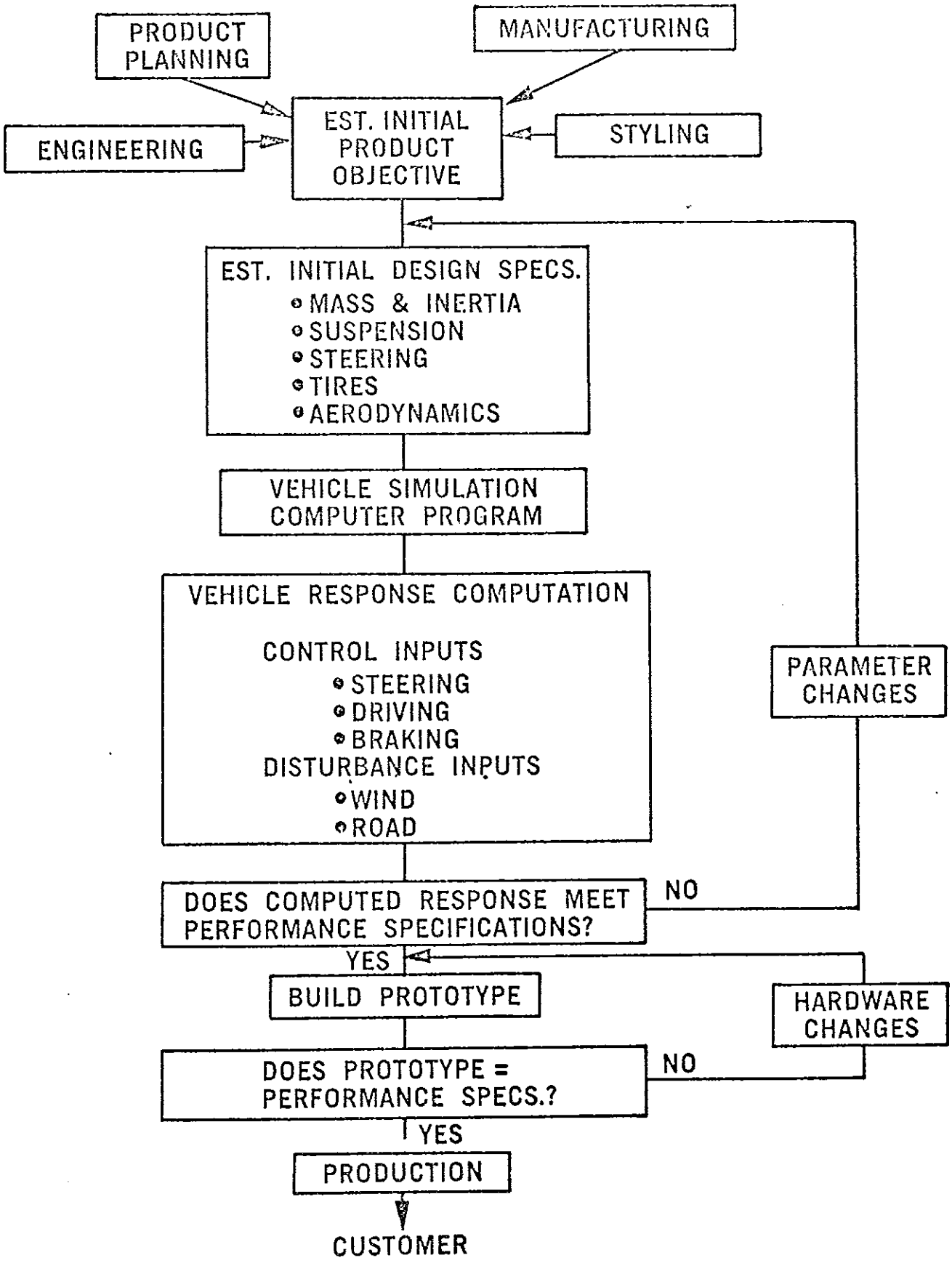

Figure 21

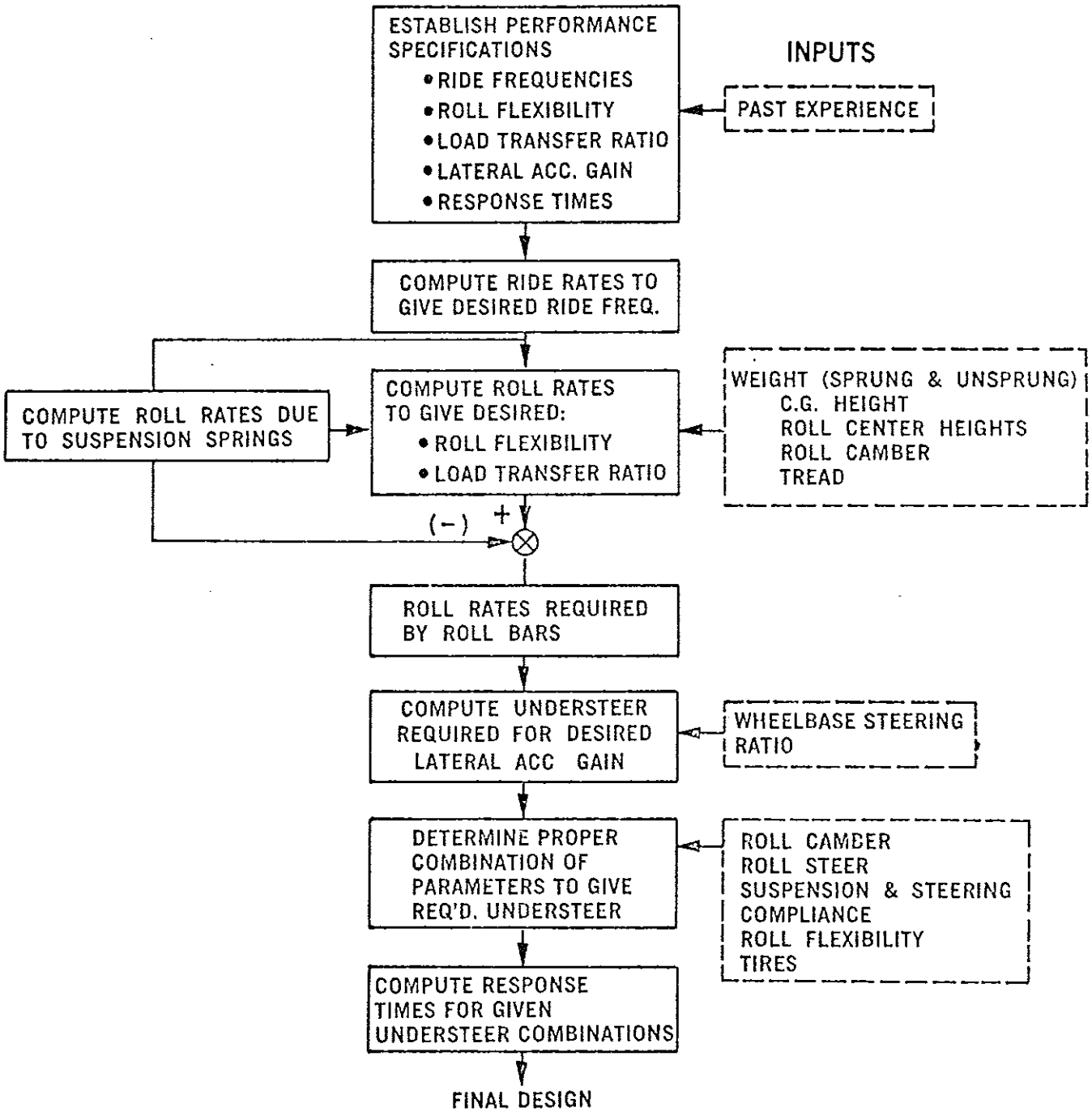

Figure 22

Development of Design Specifications for a New Model Year

The first step is to establish performance specifications as described in Figure 22. These values are determined from past experience and will be subject to change as new experience is gained.

From the ride frequencies used on equivalent previous models, it is possible to calculate the ride rates required to give similar frequencies for the subject model. The ride rates will determine required spring rates.

In the same manner, knowing the roll flexibilities and load transfer ratios of previous models, the engineer has basis for computing the required roll rates to give similar roll characteristics for the subject model. Equations 11 and 12 can be used for these computations. These roll rates represent the total required roll rates. The amount of roll rate obtained from the suspension springs can then be calculated. The difference between the required total roll rates and the roll rates due to the suspension springs defines that portion, if any, of the total roll rate that must be provided with a roll bar. Within package limitations, roll center heights can be adjusted to minimize roll bar requirements. However, adjusting roll centers can change other geometry characteristics (roll camber, roll steer) which will affect the understeer and must be kept in mind.

Once the roll characteristics have been determined, the understeer required to produce the specified lateral acceleration gain characteristics for a given wheelbase and steering ratio can be computed from equation 15.

Using the roll flexibility determined earlier, one can use the various combinations of roll camber, roll steer, suspension and steering complaince to compute the total vehicle understeer with a given set of tires (equation 10). These parameters can be adjusted within package limitations to obtain the desired value of understeer.

At the same time that the understeer is being computed, the transient response times should also be computed so that the combination of parameters will give the proper balance between steady state and transient response characteristics.

As experience is gained in making these computations, the effects of the various design parameters on the indexes of performance will become more clear and the selection of design parameters will become a logical procedure.

This procedure, described in this paper, includes only those performance indexes which are well acknowledged and primarily cover only the condition for steer inputs. As research in handling progresses, indexes of performance for traction and braking effects, wind and road disturbance inputs will evolve and become a part of the performance specifications.

STATION WAGON ANALYSIS

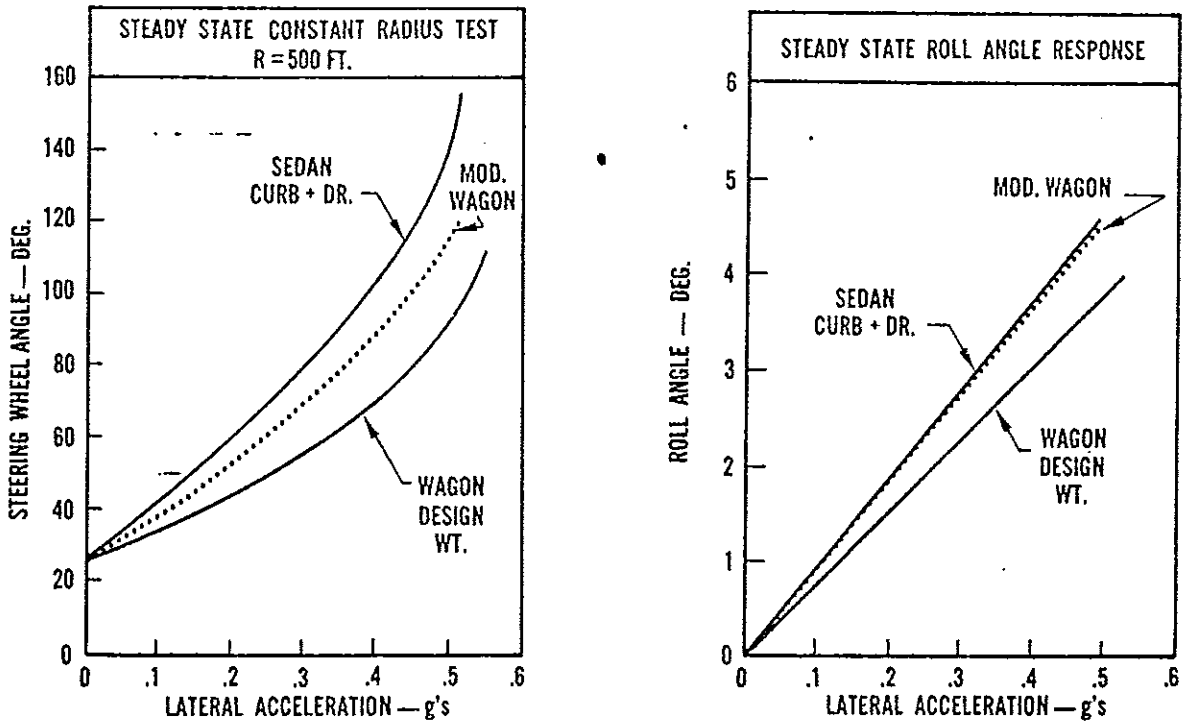

	SEDAN	WAGON	MOD.
UNDERSTEER DEG/g	8	4.1	6.8
ROLL FLEX. DEG/g	9.4	6.9	9.4

Figure 23

Station Wagon Handling Analysis

The objective of the analysis described below was to determine the difference in steady state and transient response characteristics between a sedan and a station wagon and then explore design changes that would give the station wagon response characteristics similar to the sedan. Both sedan and wagon have identical SLA independent front suspensions and solid axle rear suspensions.

Figure 23 presents a comparison of the understeer and roll flexibility characteristics of a sedan and a station wagon. As described in a preceding section, the understeer is defined as the slope of the steering wheel angle vs lateral acceleration curve for a constant radius maneuver. The roll flexibility is the slope of the roll angle vs lateral acceleration curve.

As illustrated by the curves and the tabulated data, the station wagon has substantially less understeer than the sedan (4.1 deg./g. vs 8) and the roll flexibility of the station wagon is lower than the sedans, (6.9 deg./g. vs 9.4).

Figure 24 illustrates the transient yawing velocity and lateral acceleration response to a step steer angle input. As shown, the response times for the station wagon are longer than for the sedan, for both the yawing velocity and lateral acceleration.

Two minor modifications in the station wagon produced a measurable improvement in handling performance. Roll rates were reduced to increase the station wagon roll flexibility to that of the sedan, and rear suspension roll understeer was increased. Increasing the roll flexibility produced a significant increase in total understeer by

STATION WAGON ANALYSIS

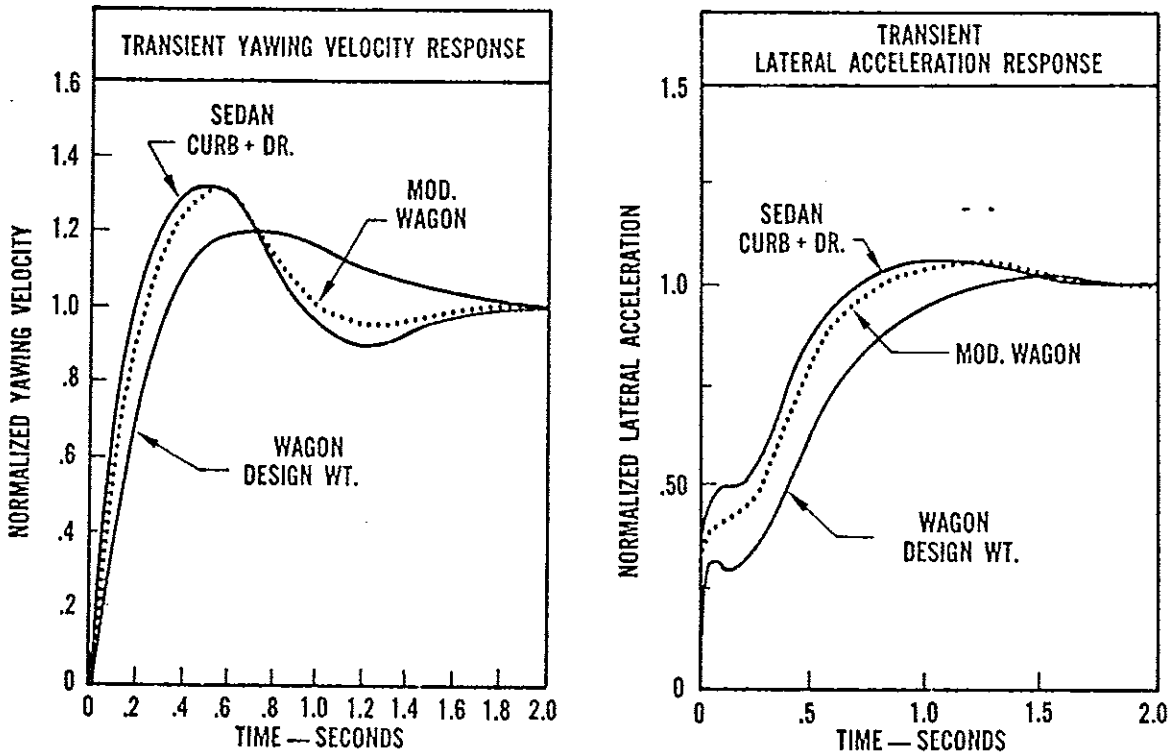

	SEDAN	WAGON	MOD. WAGON
RESPONSE TIME (SEC.)			
YAWING VELOCITY	.168	.272	.20
LAT. ACCELERATION	.43	.857	.596

Figure 24

increasing the components of understeer due to front suspension roll understeer, plus the added benefit of an increase in rear roll understeer.

This increase in understeer and roll flexibility also produced a significant reduction in the station wagon response times. Note the larger magnitude of yawing velocity overshoot of the sedan and the modified wagon as compared with the regular wagon.

Rear Suspension Comparison

(Swing Axle vs Semi-Swing vs Solid Axle)

The objective of the comparison reported next was to assess the relative handling performance of a vehicle with three alternative rear suspensions — swing axle, semi-swing, and solid axle. Both a steer and a road bump input were studied. A six degree of freedom simulation was used for the computations.

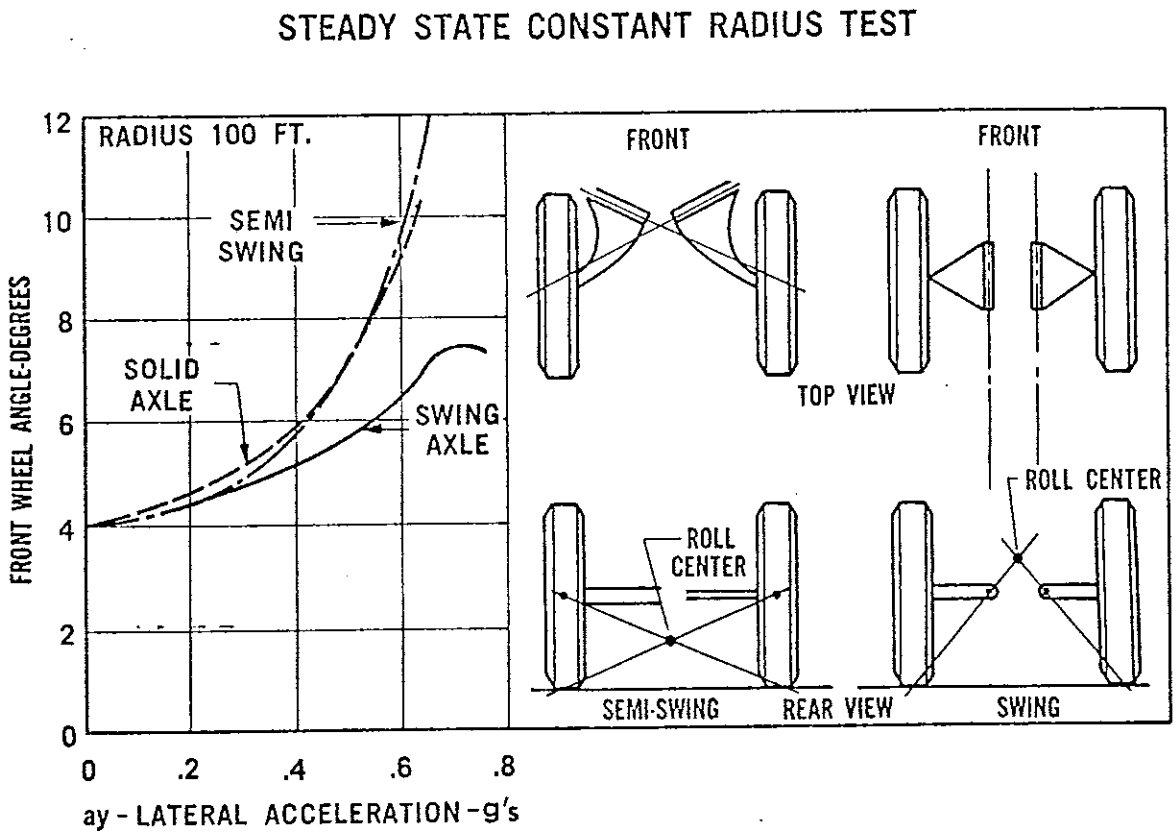

Figure 25

Figure 25 describes schematically the full swing and semi-swing axle arrangements. The pivot axis of the full swing is parallel with the longitudinal axis of the vehicle; whereas, the pivot axis of the semi-swing is skewed towards the front of the vehicle, giving a partial trailing arm effect. One of the principal effects is to lower the roll center from above axle centerline to below, as shown in the rear views.

Also presented in Figure 25 are the understeer properties of vehicles with the three subject rear suspensions. It is assumed, except for the rear suspensions, that all other vehicle parameters are the same. Note that all the vehicles are understeered at the low g lateral accelerations, but the increasing understeer of the swing axle vehicle reverses to an oversteer or spin-out condition near its maximum lateral acceleration. The solid axle and semi-swing vehicles show increasing understeer up to their maximum lateral acceleration.

Results from the computer simulation show that the change to oversteer that occurred on the swing axle vehicle is due to the jacking up of the rear suspension. Figure 26 compares the rear jack-up of the swing and semi-

STEADY STATE REAR SUSPENSION JACK UP

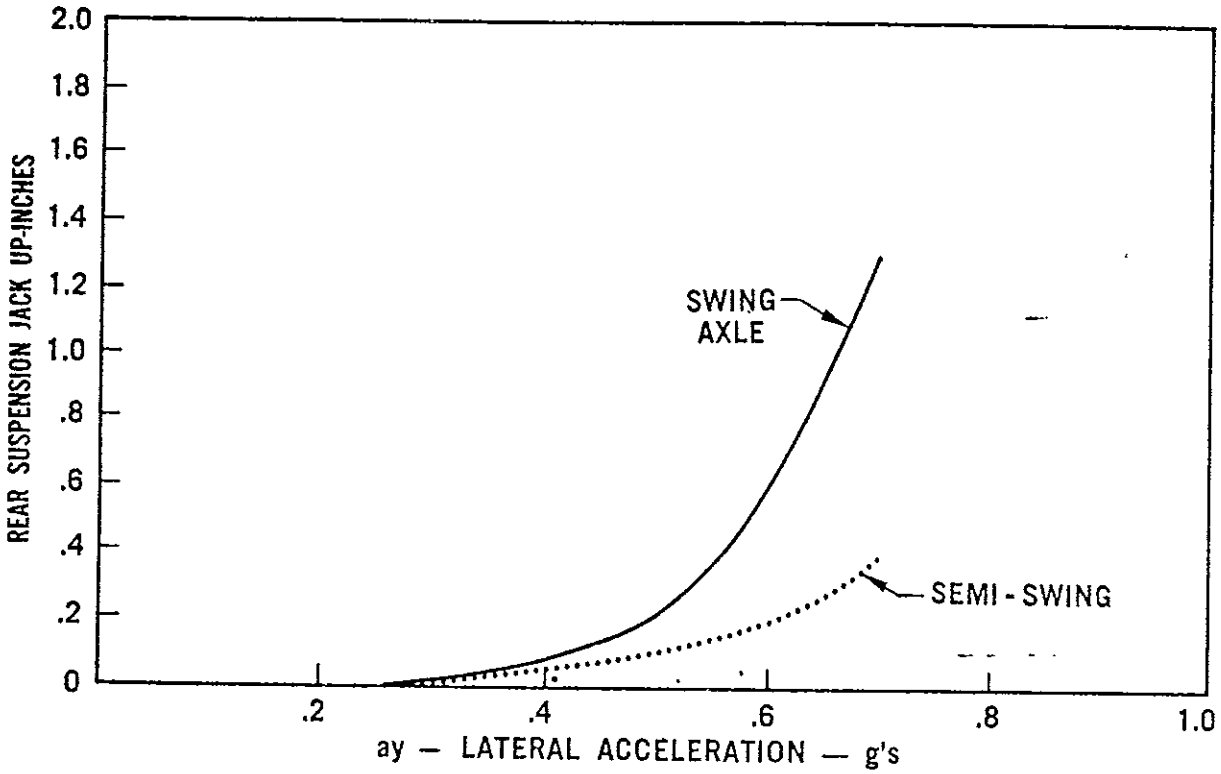

Figure 26

STEADY STATE REAR ROLL CAMBER CHARACTERISTICS

SWING AXLE VS SEMI-SWING DESIGN LOAD CONDITION

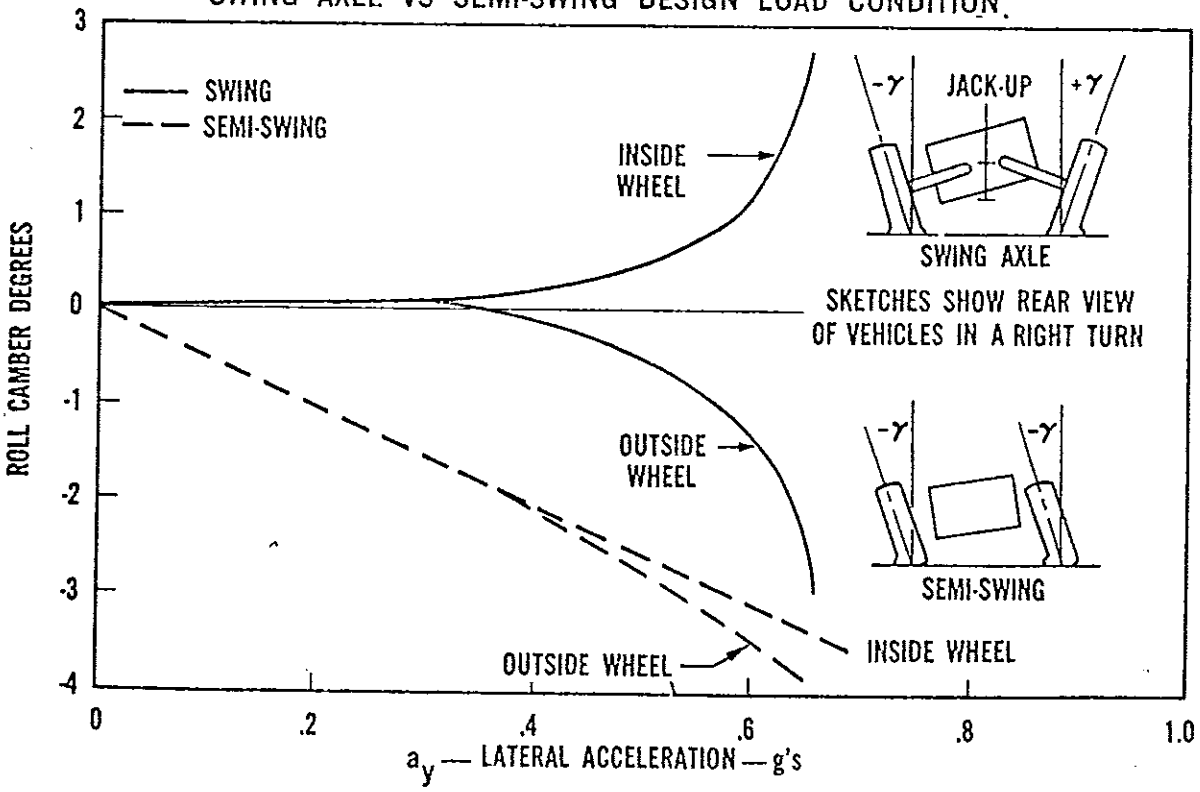

Figure 27

swing. The solid axle has no jack-up. As shown, both vehicles experience jack-up but the swing axle shows a substantially larger magnitude, with a very rapid rate of increase above .5g lateral acceleration.

Figure 27 compares the roll camber characteristics of the swing and semi-swing axle designs. Under low lateral accelerations, the roll camber of the swing axle is very small and leans toward the center of turn, which is an understeering effect. However, at the higher lateral acceleration the rapid increase in jack-up causes the outside wheel to camber toward the outside of the turn (oversteering effect) and the inside wheel cambers toward the center of turn (understeer effect). As the lateral acceleration increases, the outside wheel progressively attains a higher loading and therefore, the oversteering camber effect of the outside wheel will rapidly increase, causing the vehicle to change from an understeered condition to an oversteered condition and resulting in spin-out.

The roll camber of the semi-swing design is an oversteering effect but because it increases gradually with lateral acceleration and does not change its effect, it does not promote instability and spin out. Although the roll camber characteristic of the semi-swing design is an oversteering effect, it is possible to compensate for this oversteer with the understeer obtained from other design parameters so that the total vehicle is still understeered, as shown in Figure 25.

Figure 28 shows the transient response of the subject vehicles to a one-inch bump input on the right side of the vehicle. The shape of the bump is illustrated on the graph. Vehicle speed was 30 mph.

As shown, the response of both the swing and semi-swing design is significantly less than the solid axle design. The principal reason for this is explained in Figure 29, where the roll camber of each wheel is shown during the transient for the swing axle vehicle. The front roll camber of only the swing axle design is illustrated since it is very similar for the semi-swing and solid axle designs.

As the right front wheel contacts the bump, the wheel moves into jounce and tends to camber in the negative direction. At the same time, the front end begins to rise and roll to the left, causing the left front wheel

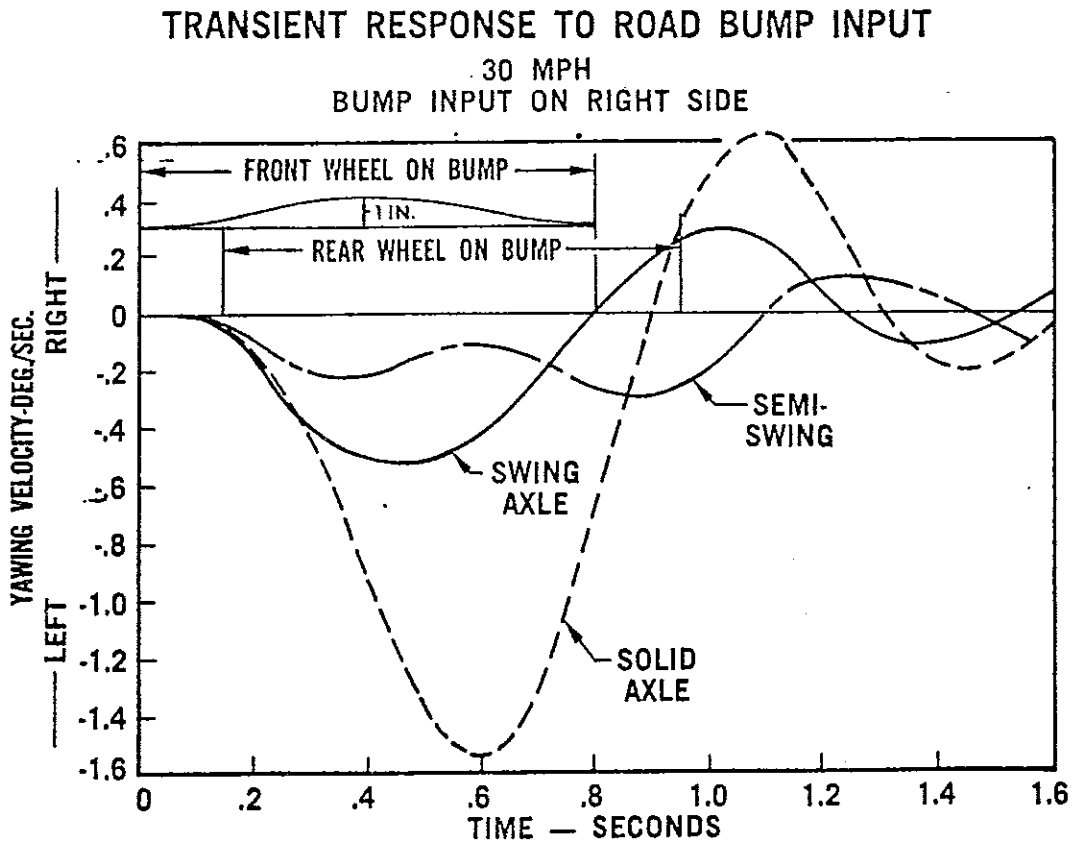

Figure 28

also to attain a negative camber. With both wheels attaining a negative camber at the same time, the combined camber thrust of both wheels is exerted on the front of the vehicle in a negative direction (to the left) causing the vehicle to yaw to the left. This occurs on all the vehicles.

The rear wheels of the swing and semi-swing designs, because of their independent rear suspensions, will also attain a negative camber condition in a similar manner as the front wheels, with only a slight time lag. The roll induced by the right front wheel also affects the rear wheels and the roll is further excited when the right rear wheel contacts the bump.

The negative camber of the rear wheels also produces a combined negative camber thrust on the rear of the vehicle (to the left) almost simultaneously with the front, but with a slight time lag. This rear thrust, combined with the front thrust, tends to minimize the yaw moment acting on the vehicle.

For the case of the solid axle design, however, there is no rear roll camber and, therefore, no counterbalancing force for the front camber thrust, resulting in a significant yaw moment disturbance to the vehicle. This results in a significantly larger yawing velocity response for the solid axle vehicle (a maximum of 1.54 deg./sec. for the solid axle vs .53 for the swing and .30 for the semi-swing).

These results would tend to indicate that vehicles with independent front and rear suspensions would be less sensitive in yaw to road bump inputs.

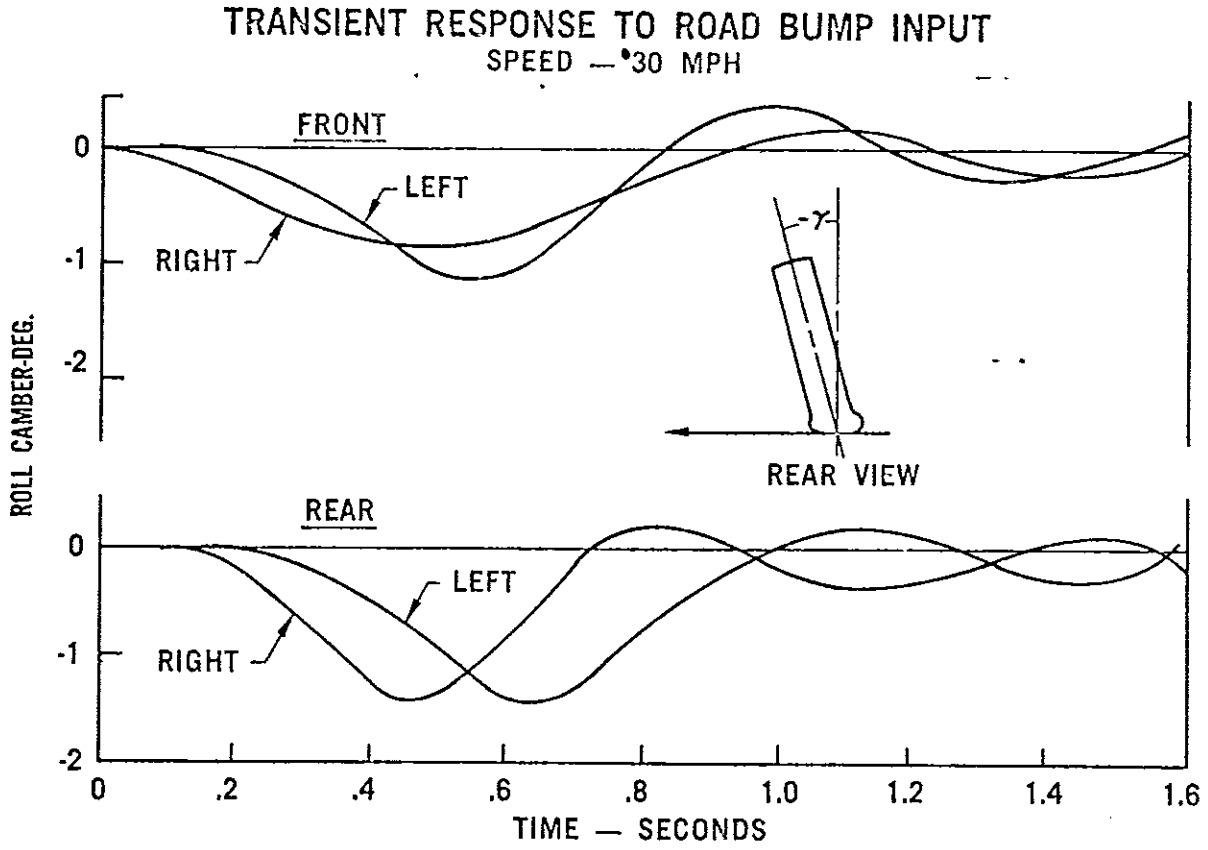

Figure 29

SUMMARY

The equations of motion for a 2 degree of freedom simulation are developed to illustrate the procedure for developing a mathematical model. The various steady state and transient indexes of performance that have been found useful in design and development are explained. The procedure for applying these prediction techniques to the design and development process are described along with specific example applications.

Experience has shown that the computed indexes of performance show correlation with observations of development engineers. As these measures are more widely used in the design and development process, they will take on increased significance and help to clarify the nebulous relation to subjective opinion. As research in handling progresses, additional indexes of performance for traction and braking effects, and wind and road disturbance inputs will evolve and become a part of the handling design process.

ACKNOWLEDGEMENT

The author wishes to express his gratitude to Mr. Bernard Los for his many contributions to the text and his assistance in the reviewing and checking of the final draft.

NOTATION

a — Distance from front axle to c.g.

a_y — Lateral vehicle acceleration

A — Lateral compliance steer

AT — Aligning torque stiffness

b — Distance from rear axle to c.g.

c — Distance from c.g. to center of pressure of cross wind force

C — Tire cornering stiffness

h_s — Vertical distance from c.g. of sprung mass to roll axis

h_u — Vertical distance from c.g. of unsprung mass to ground

I_z — Yaw moment of inertia

k — Radius of gyration

K — Roll rates

K_{ss} — Steering system compliance

l — Wheelbase

M — Mass of the vehicle

n — Steering ratio

r — Yawing velocity

R — Radius of turn

R_w — Wheel rolling radius

s — Laplace operator

S — Camber stiffness

t — Tread

t_r — Response time

U — Understeer coefficient

v — Lateral velocity of center of gravity

V — Forward speed

W — Total vehicle weight

W_s — Weight of the sprung mass

W_u — Weight of the unsprung mass

Y — Cornering forces

z — Roll center height

α — Tire slip angle

δ — Front wheel steer angle

θ_{sw} — Steering wheel angle

ϕ — Vehicle roll angle

$d\gamma/d\phi$ — Roll camber

ΔZ — Load transfer

β — Sideslip angle

ξ — Caster angle

ζ — Damping ratio

ω_d — Damped natural frequency

ω_n — Undamped natural frequency

Subscripts: 1 — front, 2 — rear

REFERENCES

1. McRuer, D. T., and Krendel, E. S., *Dynamic Response of Human Operators,* Wright Air Development Center, Ohio, WADC Technical Report J-6-524

2. Weir, D. H., and McRuer, D. T., *A Theory for Driver Steering Control of Motor Vehicles,* Paper No. 65, 47th Annual Meeting, Highway Research Board, January, 1968

3. McRuer, D.T., and Krendal, E. S., *The Human Operator as a Servo System Element,* Journal of the Franklin Institute, Vol. 267, No. 5, May and No. 6, June 1959

4. Iacovoni, D. H., *Vehicle-Driver Simulation for a Cross Wind Disturbance Condition,* SAE Paper No. 670609

5. Perkins, C. D., and Hage, R. E., *Airplane Performance Stability and Control,* John Wiley and Sons, Inc., NY

6. Nordeen, D. L., *Analysis of Tire Lateral Forces and Interpretation of Experimental Tire Data,* SAE Paper 670173, January 1967

7. Iacovoni, D. H., *The Effects of the Steering System on Directional Vehicle Stability,* Master's Thesis, Wayne State University, 1964

8. Segel, L., *Theoretical Prediction and Experimental Substantiation of the Response of the Automobile to Steering Control,* Institution of Mechanical Engineers, 1956

9. Whitcomb, D. W., and Milliken, W. F., *Design Implications of a General Theory of Automobile Stability and Control,* Institution of Mechanical Engineers, 1956

10. Bundorf, R. T., *The Influence of Vehicle Design Parameters on Characteristic Speed and Understeer,* SAE Preprint 670078, January 1967